PERFORMANCE INVESTIGATION OF VECTOR CONTROLLED INDUCTION MOTOR DRIVE

A report submitted in the partial fulfilment of

the requirement for the award of the degree

of

MASTER OF TECHNOLOGY

in

ELECTRIC DRIVES AND POWER ELECTRONICS

SUBMITTED BY: PRATYUSH PANDEY

ENROLLMENT NO. - 17527012

DEPARTMENT OF ELECTRICAL ENGINEERING

INDIAN INSTITUTE OF TECHNOLOGY

ROORKEE 247667, INDIA

CANDIDATE'S DECLARATION

I hereby declare that the work carried out in this report titled "**PERFORMANCE INVESTIGATION OF VECTOR CONTROLLED INDUCTION MOTOR DRIVE**" is presented on behalf of partial fulfilment of the requirement for the award of the degree of Master of Technology in Electrical Engineering with specialization in Electric Drives and Power Electronics submitted to the Department of Electrical Engineering, Indian Institute of Technology, Roorkee, India, under the supervision and guidance of Dr. Sumit Ghatak Choudhuri, Assistant Professor, Electrical Department, IIT Roorkee.

I have not submitted the matter embodied in this report for the award of any other degree or diploma.

Date: 17 May, 2019 PRATYUSH PANDEY

Place: Roorkee **E. No.: 17527012**

CERTIFICATION

This is to certify that the above statement made by the candidate is correct to the best of our knowledge and belief.

Dr. Sumit Ghatak Choudhari
Assistant Professor
Department of Electrical Engineering
Indian Institute of Technology, Roorkee

ACKNOWLEDGEMENT

I am using this opportunity to express my gratitude to Professor Dr. S. G. Choudhuri who supported me throughout the course of this work. I am thankful for his aspiring guidance, invaluable constructive criticism and friendly advice during the seminar work. I am sincerely grateful to him for sharing his truthful and illuminating views on a number of issues related to the work.

I am also grateful to all faculty members and staff of **Electrical Engineering Department, Indian Institute of Technology Roorkee.**

Date: 17 May, 2019 **PRATYUSH PANDEY**

Place: Roorkee

ABSTRACT

Electrical Drives today have become an important part of the modern industry. The motor drives are used in very wide power range. In various applications where speed and position control is of great significance, the drives are controlled via a power electronic converter, an interface between the input power and the motor. Vector Control is becoming the industrial standards for induction motor control. The vector control technique decouples the two components of stator current: one providing the control of flux and the other providing the control of torque. The flux as well as the torque level of the machine is controlled with perpendicular components of the stator current vector in the synchronously rotating reference frame (SRRF). Thus a current control loop is usually realized which controls the stator current and calculates the necessary inverter switching states.

Power consumption of the drive and the harmonics that it injects in the supply plays an important role in the overall performance of the drive. As VCIMD load degrades thw quality of the supply line power, it is imortant to invastigate the power quality improvement techniques on the supply side of the line. The use of multipulse AC-DC converter is such a method and its use for harmonic mitigation is not costly and energy efficient. Deduction of harmonics in supply current and improve DC output as the DC link can be achieved by using these converter. Use of multipulse convertrs in various topologies, their investigation can tells us the best suitable one for a given purpose.

CONTENT

LIST OF FIGURES

CHAPTER I
INTRODUCTION

The Induction Motor has been most widely used motor in constant speed operation. It is because of its simple construction, reliability, efficiency, reduced cost, higher torque/weight ratio and reduced maintenance. For variable speed applications, DC motor have been used and not Induction Motor. DC motor needs regular maintenance of commutator and brush segments. It is desirable to merge the the advantageous characteristic of both of these motors and many such efforts have been made [1-9] to create variable speed brushless drive.

The armature and field mmf of the DC machines are orthogonal, i.e. 900 electrical apart. The electromagnetic torque is proportional to the product of field flux and armature current.

$$T_e = K\phi I_a = K' I_f I_a$$

Field flux is directly proportional to armature current. When torque is controlled by controlling armature current, the field flux linkage is not affected, hence enabling dynamic torque response.

For the above reasons, DC motor with decoupled control of torque and flux is very suitable for variable speed operations.

In the induction motor , by the control of voltage, frequency, and slip [2,4] as in v/f control, rotor resistance control etc, for the variable speed operation only the magnitude of input variable is controlled and and is called the 'scalar controls'. In the scalar control, the response of induction motor during steady state condition is good but the dynamic response is sluggish. It is so because unlike DC motor, the torque and flux is not controlled independently in this method. To solve this problem, vector control method is developed in which the torque and flux is controlled independently with the help of decoupling circuits.[3,5,6-7]. Advances in power electronics and high power solid state devices has provided induction motor with the desirable properties of DC motor.

The VCIMD is fed by converters, causing the injection of harmonics into supply current.

The current harmonics, then flow in the source and distort the voltage at the point of common coupling, which affects nearby consumers. The power quality at the point of common coupling is deteriorated. Today, the variable frequency drive are used widely and therefore the harmonic distortion generated by them is a problem. It is recommended by IEEE Standard-519 (1992) , that the value of AC-mains current THD must be less than 8%. A method to mitigate current harmonics is by increasing the number of pulses in ac–dc converters. This method use two or more converters, where the harmonics generated by one converter are cancelled by another converter, by proper phase shift. The use of multipulse AC-DC converter is such a method and its use for harmonic mitigation is not costly and energy efficient.

This thesis will try to develop multipulse converter fed vector controlled induction motor drive (VCIMD) using various multipulse converters and compare the power quality improvement with each of them.

1.1 VECTOR CONTROL IN CAGE INDUCTION MOTOR

The principle behind vector control or field oriented control (FOC) is that the flux and torque of the induction machine are controlled independently to each other, similar to a separately excited DC machine. The stator current, which is the control variable here is expressed as a d-axis component and another as q-axis component with reference to a frame of coordinate which rotates at synchronous speed, in synchronism with stator, rotor or air gap mmf vector. Among the two orthogonal components of stator current one produces the rotor field and other produces the torque. These two current components can be controlled separately and thereby the flux and torque can be regulated independently.

The vector control implementation can be explained with the help of Fig 1.1. The controller takes the reference speed w_r^* and the actual motor speed w_r as feedback signals and generates i_{ds}^* and i_{qs}^* which are the direct and the quadrature components of the stator current vector i_s in the synchronously rotating reference frame. These two quadrature currents components are used to control flux and developed torque separately. The quadrature component are used to generate three phase reference currents, i_{as}^*, i_{bs}^* and i_{cs}^*. These reference currents are then used for inverter control which is operating in current

controlled mode and the winding currents, i_{as}, i_{bs} and i_{cs} are the feedback signals for current controller. The inverter currents i_{as}, i_{bs} and i_{cs} follow reference currents i_{as}*, i_{bs}* and i_{cs}*. The winding currents are transformed into synchronously rotating reference frame as i_{ds} and i_{qs} which are made follow the set quadrature currents i_{ds}* and i_{qs}*. An inverter with fast current regulation capability is desirable here. The motor currents in the vector control are controlled quickly. Dynamic performance of drive in the vector control therefore is very good.

The accurate information about the magnitude and position of rotor flux is required for decoupling of flux and torque control. The accurate position of rotor flux can be obtained from flux sensors or by using flux estimators. Flux estimator computes the flux vector from stator voltage and current or from speed sensor signal or from both.

1.2 DIRECT AND INDIRECT VECTOR CONTROL OF INDUCTION MOTOR

There are two types of vector control that can be employed, direct control and indirect control. The method used to access the rotor flux is different in both of them. In the direct vector control, rotor flux vector is measured using flux sensors like Hall-effect sensors. It is also termed flux feedback control. Using sensors is expensive because special modifications of the motor are required for placing the flux sensors. At low speed due to the dominance of stator resistance voltage drop in the stator voltage equation, this limiting operation of drive down to zero. Inaccuracies are also found and due to variations on flux level and temperature. Knowledge of rotor flux position is very important in FOC. The flux model can not compute the rotor flux vector accurately because of the harmonics present in the stator currents and voltages. It is because of these disadvantages direct vector control is not used, indirect vector control is used. In indirect vector control technique,flux sensors are not used. [2]

Indirect vector control is also called flux-feedforward control or slip frequency control. The rotor flux vector is computed from the speed feedback signal of the motor. [4,6] It requires high resolution rotor speed or position sensor for accurate measurement of rotor flux vector position. The difference between the rotor speed and reference speed is given to controller. The slip speed of motor is computed and synchronous speed is obtained. The

rotor flux vector is also rotating with synchronous speed and from this the position of rotor flux vector can be estimated.

Here, therefore, the indirect vector control method will be used with rotor flux orientation as it is simpler than stator flux orientation for induction motor supplied by impressed stator current.

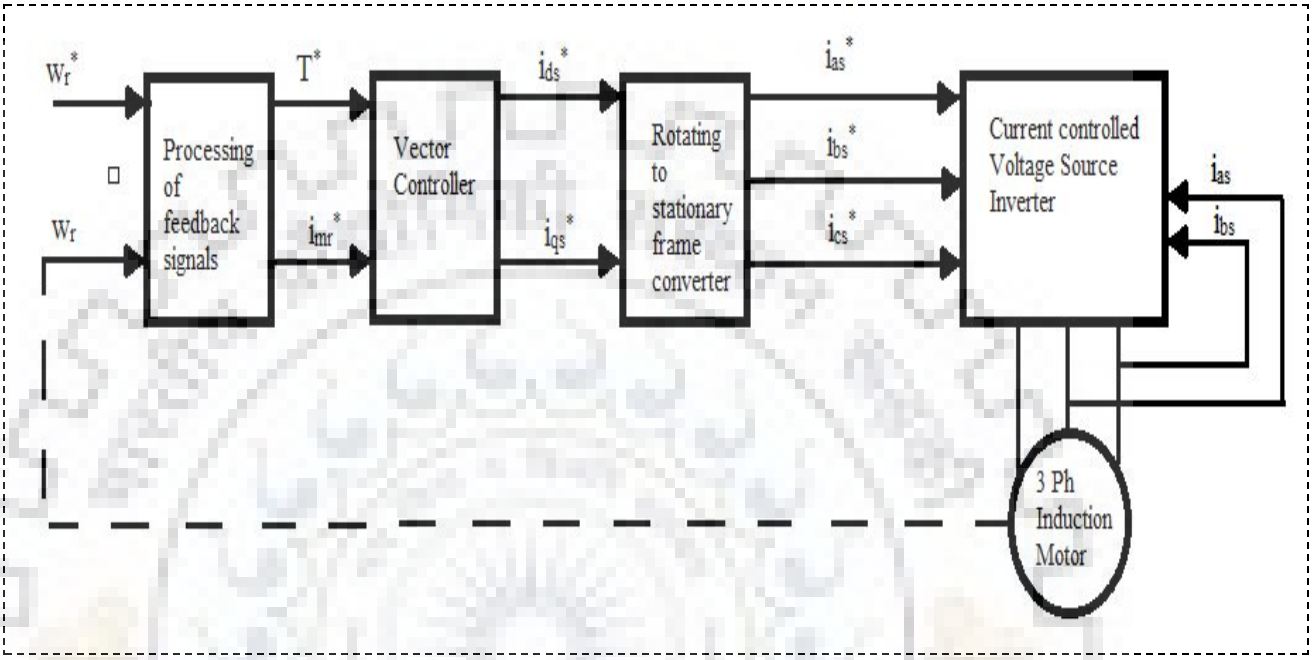

Fig 4.2 Block Diagram of Indirect Vector Control Induction Motor Drive

1.4 CHAPTER OUTLINE

Chapter 1

This chapter includes concept and importance of VCIMD. It explains how the induction motor is operated similar to the separately excited dc motor. It contains the literature review of different literature available on the subject matter.

Chapter 2

In this chapter, the description of vector controlled induction motor drive and its modelling is done. The modelling is done mathematically and is simulated in the Matalab. Detail expressions and relations among equations is given.

Chapter 3

This chapter presents the simulation results of VCIMD under various operating modes, such as, start mode, brake mode, reversal of speed, step change in speed command, the simulated results are then shown accordingly.

Chapter 4

In this chapter, the converter inverter arrangement was utilised to feed VCIMD to reduce the harmonics generated and improve the power quality of the supply side. Multipulse cnoverters are discused and there design is investigated in details.

Chapter 5

In this chapter, the performance results of vector controlled induction motor dirive fed by various multipulse converters are observed and conclusion drawn. It presents detail simulation report and on different topologies investigated.

CHAPTER II

DESCRIPTION OF VECTOR CONTROLLED INDUCTION MOTOR DRIVE SYSTEM

Separately excited DC motor has linear control plant and decoupled control structure facilitating independent control of flux and torque. On the other hand, induction motor has a non-linear and highly interacting multivariable control plant. With the help of vector control the dynamic structure of induction motor is changed in such a way that its performance is similar to the separately excited DC motor. Vector control method has enabled the use of cage induction motor in application where earlier only DC motor was found appropriate [3]. An induction motor is when compared with a DC motor for same application is smaller, mechanically more rigid, less expensive and because it does not have commutator and brushes it requires less maintenance.

An induction motor is controlled like a separately excited DC motor in vector control method. In fully compensated DC motor, the magnetic field is established by stationary poles. The stationary poles is produced either by permanent magnet or DC excited field winding. The armature rotates in the established magnetic field. When the current is given to the armature through the commutator, the armature mmf field is produced which is a quadrature with the main field axis. The main field mmf and armature mmf thus have orthogonal relationship and is independent of the rotation speed.

In the induction motor, the space angle between rotating stator and rotor field is dependent on the load. It changes with the change in load causing oscillatory dynamic response. The space angle if controlled, the stator input current can be decoupled into flux-producing and torque-producing components. It is done using vector control, which creates about 90^0 space angle difference between specified field components. Using this, the induction motor gives similar characteristics as that of a separately excited DC motor.

2.1 DC MOTOR ANALOGY

The analogy between vector control induction motor and DC motor can be explained through Fig. 2.1.

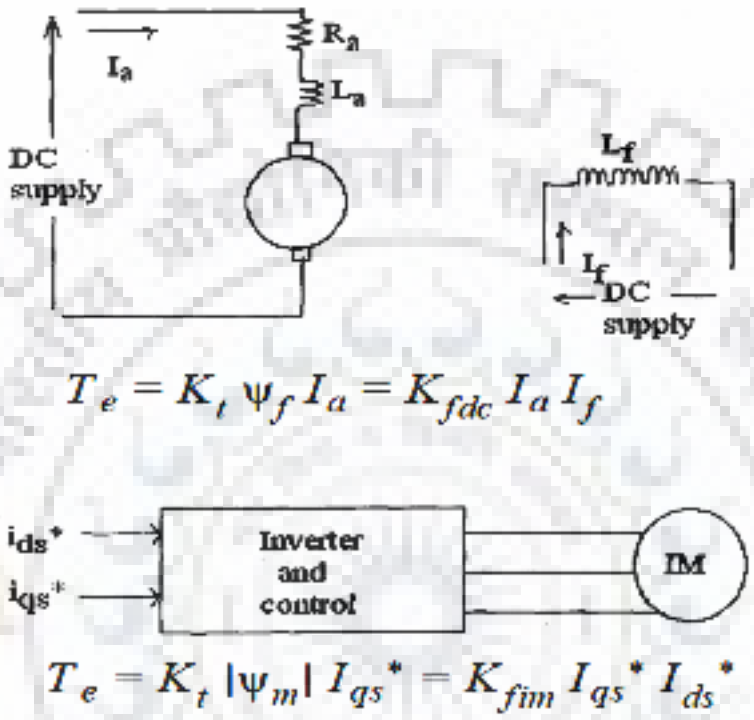

Fig. 2.1 Induction Motor Analogy with DC Motor in Vector Control

The torque in a fully compensated DC motor is given by,

$$T_e = K_{fdc} I_a I_f \tag{2.1}$$

Where, K_{fdc} is the torque constant of the DC motor,

I_a is the armature current and,

I_f is the field current.

The angle between I_a and I_f is independent of both speed of the motor and load on the saft and is 90^0. These two are independent control variables. The current I_f which produces flux and the current I_a which produces torque is separately controlled and is independent from each other. It provides fast dynamic response through quick control of the developed electromagnetic torque both in transient and steady state condition. When we control induction motor in a synchronously rotating reference frame, the sinusoidal quantities of the motor becomes dc quantities and induction motor can be controlled like DC motor [6].

In the Fig. 2.1, the induction motor with inverter and control is shown, it has two inputs, i_{ds}* and i_{qs}*. The current i_{ds}* is direct axis current component of the stator current and is analogous to field current I_f and i_{qs}* is quadrature axis current component of the same and is analogous to armature current I_a. Both are expressed in synchronously rotating reference frame. Therefore, i_{ds}* and i_{qs}* are flux producing and torque producing component of stator current vector respectively. The torque in the induction motor is given by,

$$T_e = K_{fim} I_{qs}^* I_{ds}^* \quad (2.2)$$

where, K_{fim} is torque constant of the induction motor,

I_{ds}^* is flux producing component of stator current vector and,

I_{qs}^* is torque producing component of stator current vector.

The induction motor torque expressed in the above equation (2.2) is identical to the torque equation of DC motor (2.1). The angle between i_{ds}* and i_{qs}* is independent of both speed of the motor and load on the saft and are independent control variables. This fulfills the condition of the vector control.

For below the base speed in normal operating condition i_{ds}* is kept constant and torque is changed by controlling i_{qs}* , a behaviour similar to separately excited DC motor. The currents i_{ds}* and i_{qs}* are controlled separately in the flux control loop and torque control loop, respectively.

2.2 BASIC MODEL OF THE DRIVE SYSTEM

In an induction motor the torque is produced by interaction of current in the rotor conductor with the magnetic flux density in the air gap to which the rotor is subjected. Unlike DC motor, in the induction motor all inputs are given to the stator only. The current in the stator is responsible for both inducing current in the rotor conductor and creating magnetic field in the airgap [5].

In the vector control, the components producing flux and torque is seperated and controlled independently. The basic model of vector controlled induction motor drive system is shown in Fig 2.2.

The system has two control loops, which are the flux control loop and torque control loop. The closed loop controller compares the torque component with the demanded torque and

makes necessary changes to make torque component equal to the demanded torque. Similarly, The flux controller compares the flux component with the reference field. The field reference has constant value for all speeds below base speed. For speeds above base speed the reference value of flux is reduced. The controller makes necessary changes to make field component equal to the reference field. We get i_{ds} from the flux control loop and i_{qs} from the torque control loop. These two currents are orthogonal and DC in nature. These two current quantities are processed in the field oriented control structure of the motor along with the feedback signals obtained from winding current and voltages, rotor speed and fluxes etc. This control structure gives control commands to the inverter switch (ON/OFF signals). The inverter supplies the currents through the motor whose stator current vector components depends on their set references which are flux and torque requirements in the drive. Thereby, enabling fast dynamic response.

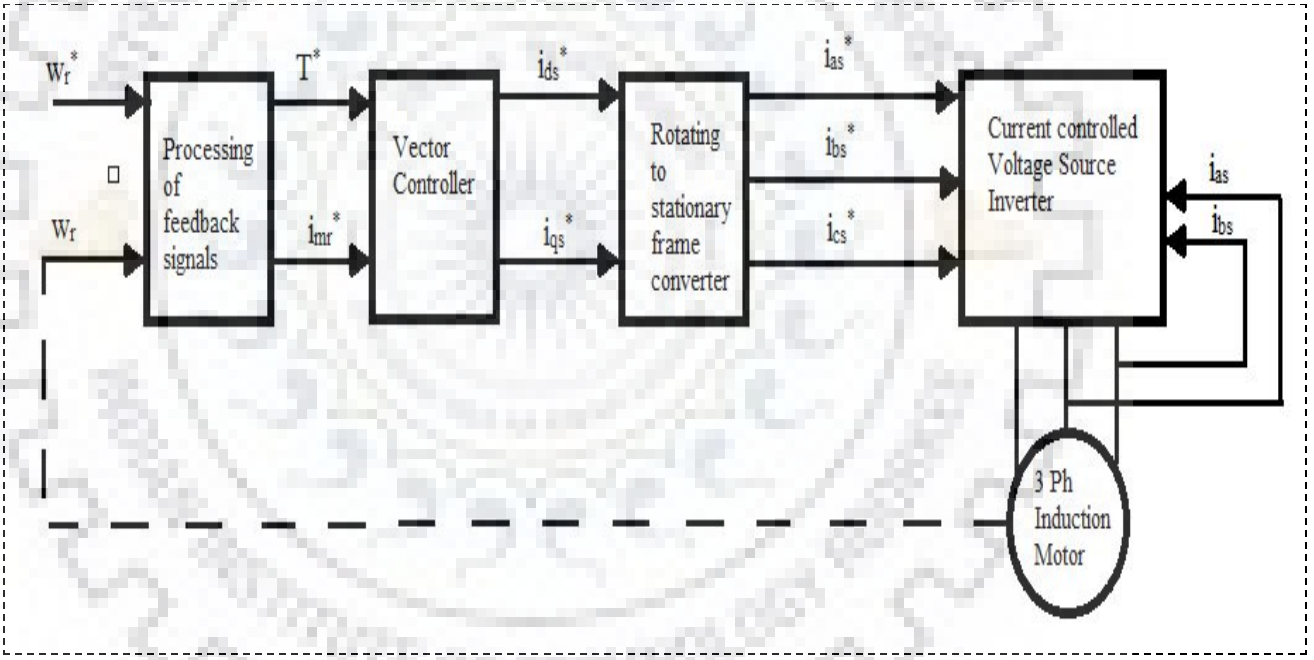

Fig 2.2 (a) Model of Vector Controlled Induction Motor Drive

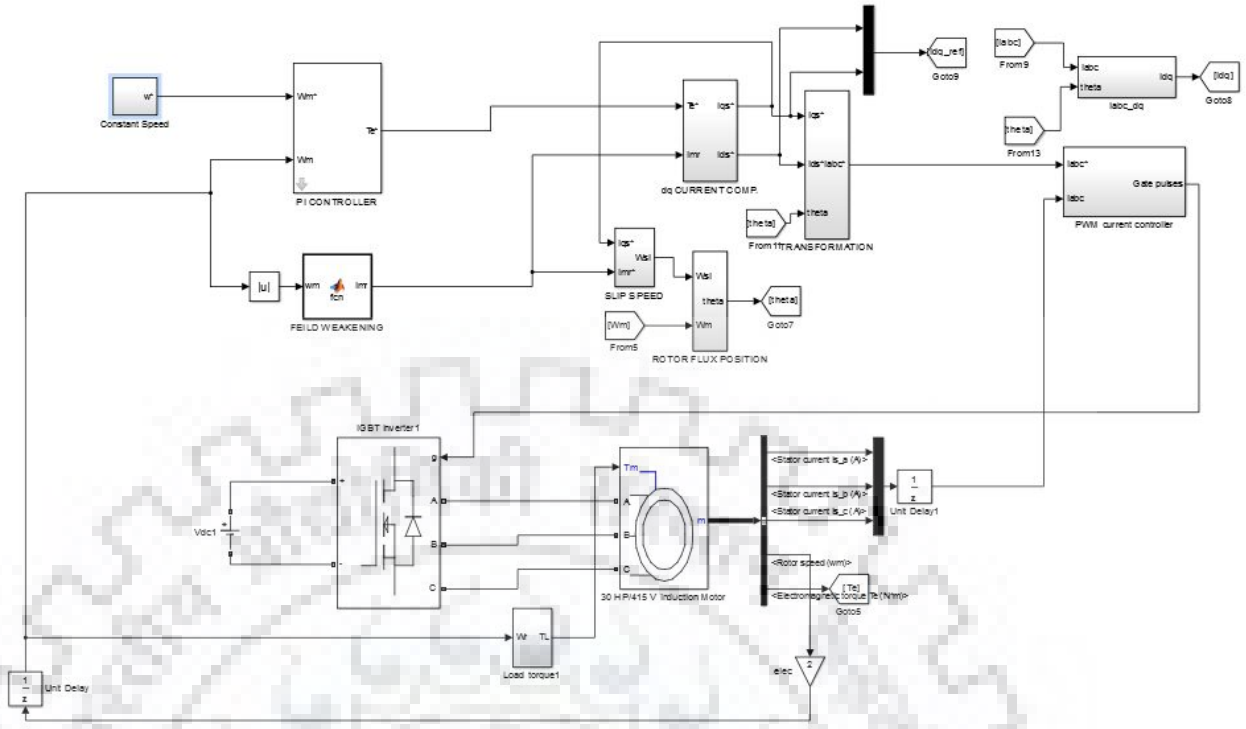

Fig 2.2 (b) Model of Vector Controlled Induction Motor Drive in MATLAB frame

2.3 SPEED SENSORS

In the vector control of induction motor, very precise measurement of speed and position of the rotor flux vector is required. To accomplish this, a high resolution and high precision sensor is needed. For the the cage induction motor's closed loop vector control, shaft encoders are used.

2.4 SPEED CONTROLLER

ω_r which is the speed measured is compared with the reference speed w_r^* and error is generated and the output speed error ω_e is given in the speed controller. The speed controller gives thesignal for control of torque command T. The speed error may be negative or positive. There are different type of speed controllers, PI, PID, Fuzzy, adaptive etc.

Speed controller is followed by a limiter which give final limited reference torque T_e^*. The speed error at n^{th} instant of time is given as:

$$\omega_{e(n)} = \omega_{r(n)}^{*} - \omega_{r(n)} \tag{2.3}$$

where, $\omega_{r(n)}^{*}$ is reference speed of the motor and

$\omega_{r(n)}$ is actual speed of the motor.

2.4.1 Proportional Integral (pi) Speed Controller

The Block diagram of PI controller is as shown in Fig. 2.3

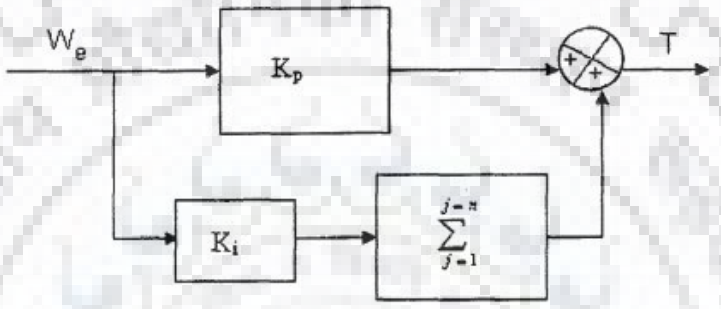

Fig 2.3 Block Diagram of PI Speed Controller

The output of controller at n^{th} instant is given as,

$$T_n = T_{n-1} + K_p\{\omega_{re(n)} - \omega_{re(n-1)}\} + K_i\omega_{re(n)} \tag{2.4}$$

where, T_n is the torque output at the n^{th} instant,

K_p and K_i are proportional and integral constants and

$\omega_{re(n-1)}$ is the speed error at $(n-1)^{th}$ instant.

The gain parameters of the PI controller are selected by the trial and error method by observing their effect on the response of the drive. Their numerical values depends on the rating of motors. (Appendix 1)

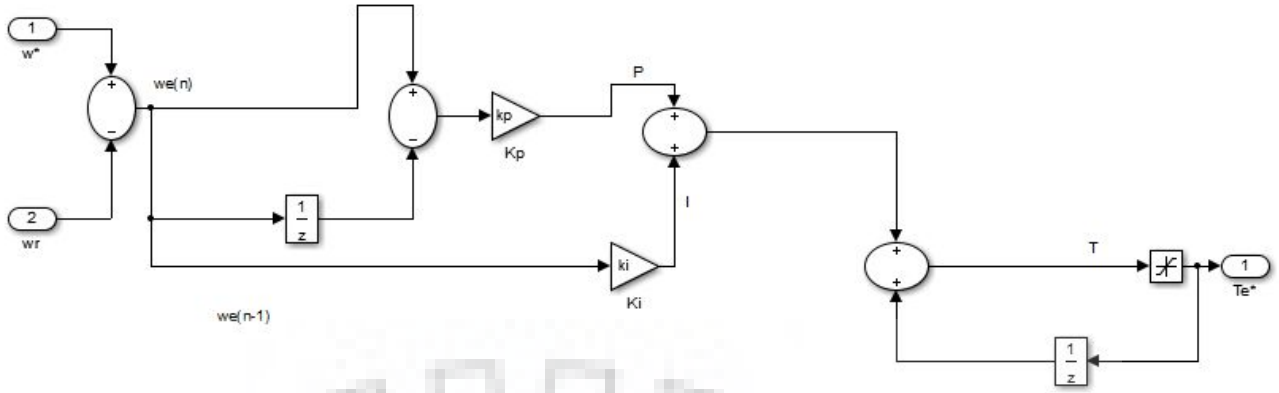

Fig 2.4 PI Speed Controller in MATLAB frame

2.4.2 Fuzzy Logic Speed Controller

The inputs to FL speed controller is e(n) and δe(n), where δe(n) is the change in the error signal. The crisp value ofboth the signal is converted into respective fuzzy variables [. The fuzzification maps the error to a language decision domain. The knowledge base defines the rules ggoverning the relationship between input and output variables in term of membership functions. A set of 'If-Then' rules is considered as control rules . The Table 2.1 shows the fuzzy logic decision table for simulated controller for VCIMD. The simulink structure in MATLAB is given in Fig. 2.5.

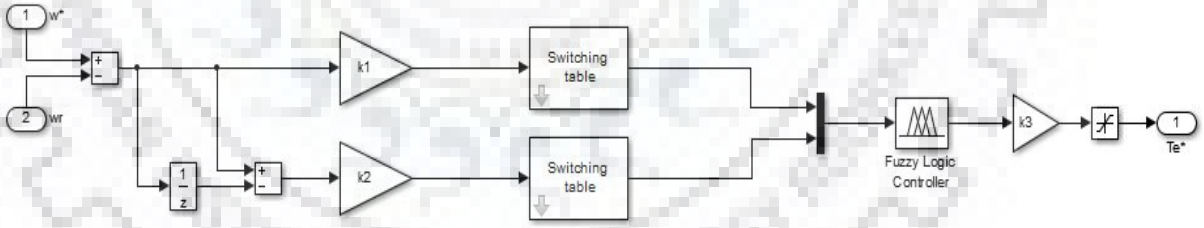

Fig 2.5 Fuzzy Logic Speed Controller in MATLAB Frame

The step by step process of FL speed controller is procesed as:

- The speed error e(n) and δe(n) is calculated and converted into per unit values.
- The FL controller takes the crisp value and changes it into linguistiv values.
- The output of the linguistic format is calculated by rule base data. Mamdani model is used.

- The output value is converted to the crisp value using centroide method.
- The crisp value output is scaled back to get the controller output.
- After limiting the controller outpur, reference torque (T*) is generated.

2.4.3 Intellligent Speed Controller

This controller combines the PI and FL ina an intelligent format and improves the system dynamics. Switching betweent the two controller is dne by using an intelligent methodology as shown in the diagram schematically in Fig. 2.6

The per unit speed is taken as a function argument in the controller. It imploys the dvantages ofboth the PI and FL controller into a one Intelligent controller.

As shown in Fig. 2.6 the switching between the two controllers is done using the scaled speed error input

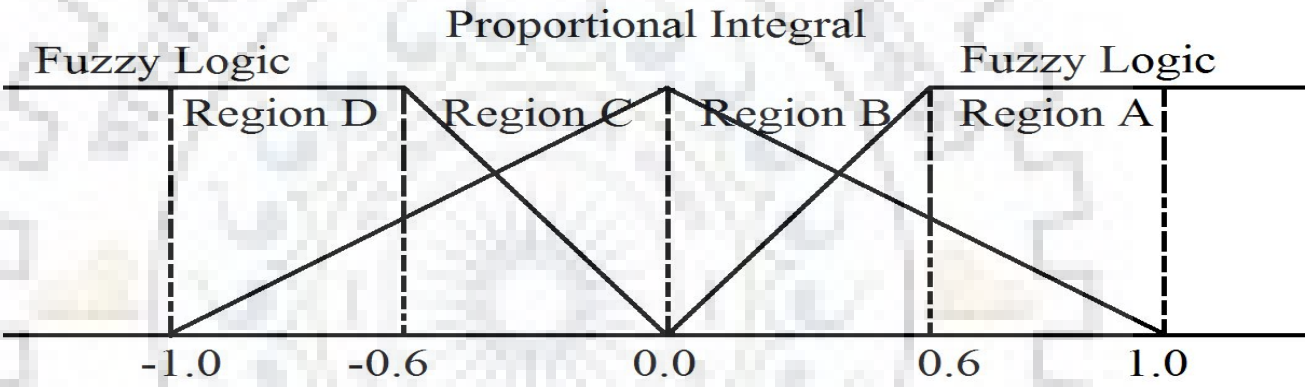

Fig 2.6 Schematic architecture of the Intelligent Speed Controller

In case speed error is more than 1.0, only Fuzzy Logic speed controller takes action. The four regions are defined as:

Region A: $W_{FL} = 1$ and $W_{PI} = 1 - \omega_{re(scaled)}$

Region B: $W_{FL} = (1/0.6)\,\omega_{re(scaled)}$ and $W_{PI} = 1 - \omega_{re(scaled)}$

Region C: $W_{FL} = (-1/0.6)\,\omega_{re(scaled)}$ and $W_{PI} = 1 + \omega_{re(scaled)}$

Region D: $W_{FL} = 1$ and $W_{PI} = 1 + \omega_{re(scaled)}$

Where W_{FL} and W_{PI} refers to the weight of FL and PI speed controllers respectively.

The resultant Torque $T_n = W_{FLn}T^*_{FLn} + W_{PIn}T^*_{PIn}$ where n = A,B,C,D

Tn is the net calculated torque of intelligent controller being fed to the limiter.

2.5 LIMITER

During the transient conditions such as when the drive operates in the starting, reversing or when there is a load perturbations the speed controller output (T) may become a very high,

for fast acheiving the steady state condition,so, the controller output orque value may become as high or higher than the breakdown torque. To avoid this, it is needed to limit the maximum torque value. Speed controller give refence Torque(T^*). As a result. the limit on the torque ensures overcurrent protection to the drive. Whenever reference speed change or there is an application of load torque on the motor shaft, the speed controller output is limited to a maximum possible value (T^*). Therefore, the limiter on the speed controller output provides an inherent stability to the closed loop speed control system.

2.6 FIELD WEAKENING CONTROLLER

This is active only when the speed goes above the rated speed. Input is the speed and out is the i_{mr} current. Below the base speed it is constant, but above the rated speed it increases with reverse proportion.

$i_{mr\,(n)}^{*} = i_m$ if $w_{r\,(n)}$ < base speed of motor

$i_{mr\,(n)}^{*} = K_f\, i_m / w_{r(n)}$ if $w_{r\,(n)}$ >= base speed of motor mr (2.5)

where K_f : flux constant

i_{mr}^{*} : excitation current,

i_m : magnetizing current,

$w_{r\,(n)}$: feedback speed of the motor drive,

w_b : base speed of the motor drive.

2.7 VOLTAGE SOURCE INVERTER (VSI)

The three phase voltage source inverter (VSI) comprises of a bridge configuration of six IGBT switches with respective freewheeling diodes. Sinusoidal PWM current controller operates the VSI in current control mode [15]. The controlled VSI forms a variable voltage source at varying frequencies for the three phase induction motor. The output voltage of the inverter depends on the combination of switching functions S_A, S_B and S_C. The three phase voltages can be expressed as:

$$V_{as}=V_{dc}(2S_A - S_B - S_C)/3 \quad (2.6)$$

$$V_{bs}=V_{dc}(-S_A+2S_B - S_C)/3 \quad (2.7)$$

$$V_{es}=V_{de}(- S_A - S_B+2S_C)/3 \quad (2.8)$$

2.8 THREE PHASE SQUIRREL CAGE INDUCTION MOTOR

The main component of the drive is the induction motor. The motor runs at the set reference speed (wr *) in the required direction and converts supplied electrical energy into mechanical energy, robust in construction and free from maintenance.

Mathematical Model of Induction Machine:

The squirrel cage induction motor is modeled using d-q theory in the stationary reference frame so that we get less number of equations and the analysis becomes easy. The voltage-current relationship in the stationary reference frame of the induction motor in terms of the d-q

variable is expressed as [2][47]:

$$[V] = [R][i] + [L]\,p[i] + \omega_r[G][i] \tag{2.9}$$

Therefore by simplifying, the current derivative vector can be expressed as follows:

$$p[i] = [L]^{-1}\{[v] - [R][i] - \omega_r[G][i] \tag{2.10}$$

where, 'p' is the differential operator $\frac{d}{dt}$ and

' ω_r ' is the rotor speed in electrical `rad/sec'.

Current and Voltage vectors are given as follows:

$$[i] = [i_{qss} \quad i_{dss} \quad i_{qrs} \quad i_{drs}]^T \tag{2.11}$$

$$[v] = [v_{qss} \quad v_{dss} \quad v_{qrs} \quad v_{drs}]^T \tag{2.12}$$

where v_{qss} and v_{dss}, are the q-axis and d-axis voltages, applied across the stator windings referred to the stator and v_{qrs} and v_{drs}, are the q-axis and d-axis voltages across the rotor windings referred to the stator. As the rotor bars are short circuited in a squirrel cage induction motor, the voltages v_{qrs} and v_{drs}, are zero. Similarly the currents are also defined. [L] is the inductance vector, [R] is the resistance vector and [G] is the rotational inductance matrix and have the usual meaning. All the voltages and currents are expressed in the stationary reference frame.

The torque balance equation is stated as:

$$p\omega_r = \left(\frac{p}{2}\right)\frac{(T_e - T_L)}{J} \quad (2.13)$$

Where T_L : load torque on motor including friction and windage losses,

T_e: developed electromagnetic torque by the motor.

2.9 MATHEMATICAL ANALYSIS OF VECTOR CONTROLLER

Reference torque (T^*) is the output of the speed controller and output of field weakening controller (i_{mr}^*) is the reference lux. The two signals are take by the Vector Contoller and torque component (i_{qs}^*) and the flux component (i_{ds}^*) of the stator current (i_s^*) is calculated. The slip frequency (w_2^*) is also calculated.

Estimation of i_{ds}^* , i_{qs}^* and w_2^*

The equations for calculating these two components of the current in the discretized form are stated as follows [2,4,14]:

$$i_{ds}^*{}_{(n)} = i_{mr}^*{}_{(n)} - \tau_r \frac{di_{mr}^*}{dt} \quad (2.14)$$

$$i_{qs}^* = \frac{T^*{}_{(n)}}{K\, i_{mr}^*{}_{(n)}} \quad (2.15)$$

$$\omega_2^*{}_{(n)} = \frac{i_{qs}^*{}_{(n)}}{\tau_r\, i_{mr}^*{}_{(n)}} \quad (2.16)$$

where τ_r , is the rotor time constant

$$\tau_r = \frac{L_r}{R_r} \quad (2.17)$$

$$K = \left(\frac{2}{3}\right)\left(\frac{P}{2}\right)\left(\frac{M}{1+\sigma_r}\right) \quad (2.18)$$

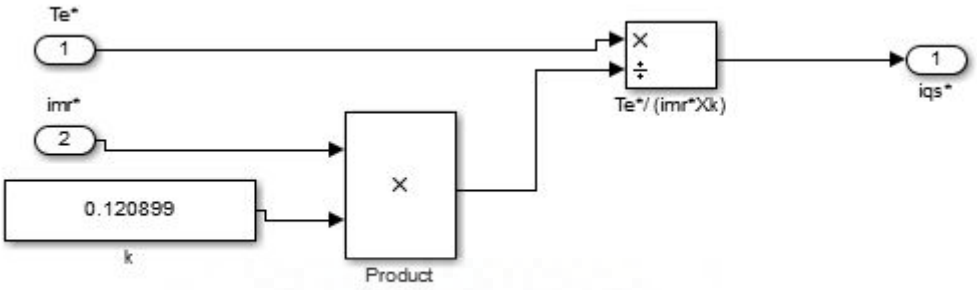

Fig 2.7 Subsytem to obtain i_{qs}^{*} from T^{*} and i_{mr}^{*} in MATLAB

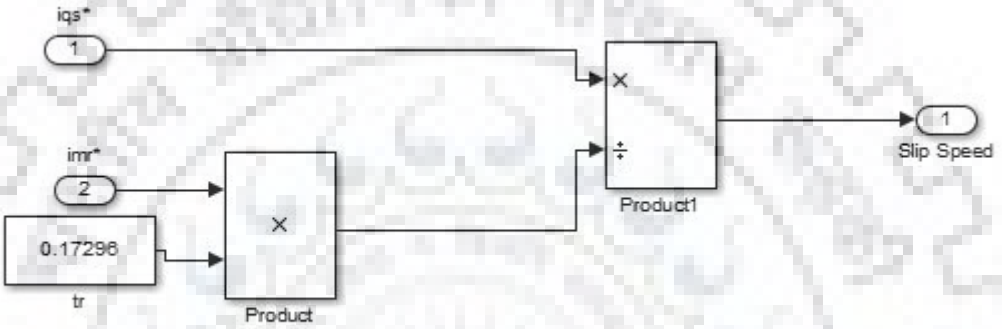

Fig 2.8 Subsytem to obtain slip speed from i_{qs}^{*} and i_{mr}^{*} in MATLAB

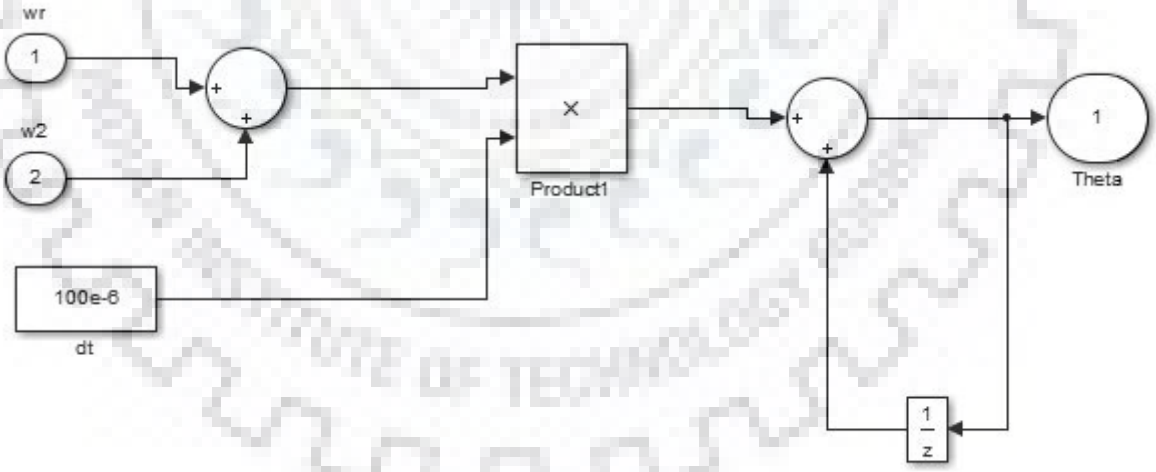

Fig 2.9 Subsytem to obtain θ in MATLAB

P = number of poles,

$i_{ds\ (n)}^{*}$ and $i_{qs\ (n)}^{*}$ are flux and torque components of stator current at n^{th} instant, $w_{2\ (n)}^{*}$ is the n^{th} instant of the reference slip speed, M is the mutual inductance, σ_r is the rotor leakage factor and L_r is the rotor self inductance which is:

$$L_r = L_{ir} + L_m \tag{2.19}$$

$$L_r = (1+ \sigma_r)M \qquad \sigma_r = \frac{L_r}{M} - 1 \tag{2.20}$$

where, $M = (3/2)L_m$,

R_r : rotor resistance ,

L_m is the magnetizing inductance.

CHAPTER III
SIMULATION RESULT

This chapter presents the simulation results of VCIMd under various operating modes. Analysing VCIMD under these operating conditions can help us test the suitability of motor in various industrial process in conveyors, fan load, feeders, pump load, etc.. The result are obtained in the Matlab using Simulink and power system blocks in discrete time frame using samping time 100 microseconds.

Rating of the motor tested is: 30HP, 3-Phase, 4-Pole, Y-connected, 239.6V, 45.0A, 50Hz.

Three different types of speed controllers are used, PI, FL and Intelligent speed controller.

3.1 VCIMD DYNAMIC RESULTS

3.1.1 START MODE DYNAMICS

The motor starts at low frequency, controlled by converter and reaches the steady state set speed of 250 electrical rad/sec. The start dynamic is shown in Fig 3.1

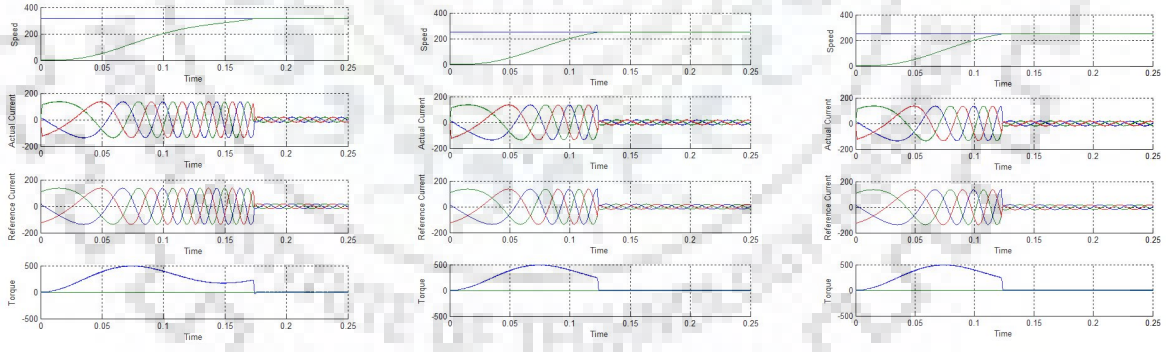

(a) (b) (c)

Fig 3.1 Starting dynamics of VCIMD with (a) PI (b) FL and (c) IC

3.1.2 REVERSAL DYNAMICS

In the reversal mode, the reference speed is brought to negative of the rated speed. Here it is -250 elec rad/sec. The dynamic is shown in Fig 3.2.

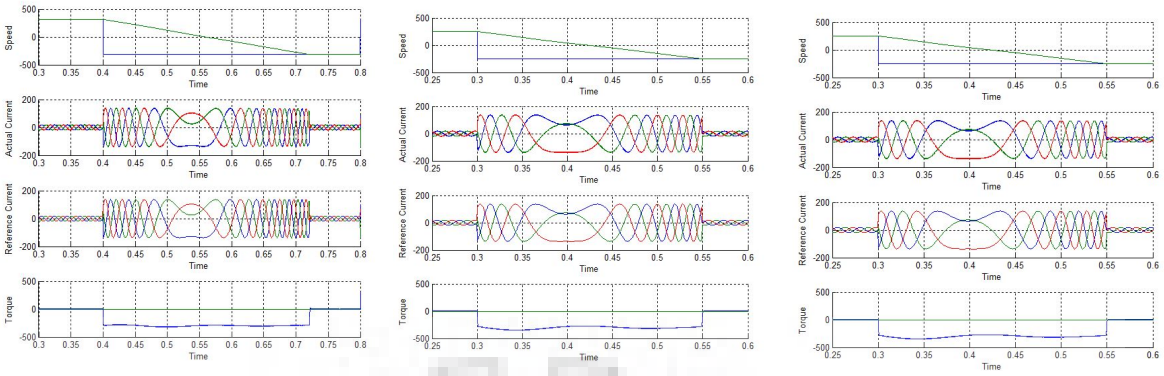

(a) (b) (c)

Fig 3.2 Revarsal dynamics of VCIMD with (a) PI (b) FL and (c) IC

3.1.3 DRIVE ON LOAD

The motor is started from rest and three types of load which are, constant, linear and quadratic loads are applied.

CONSTANT LOAD

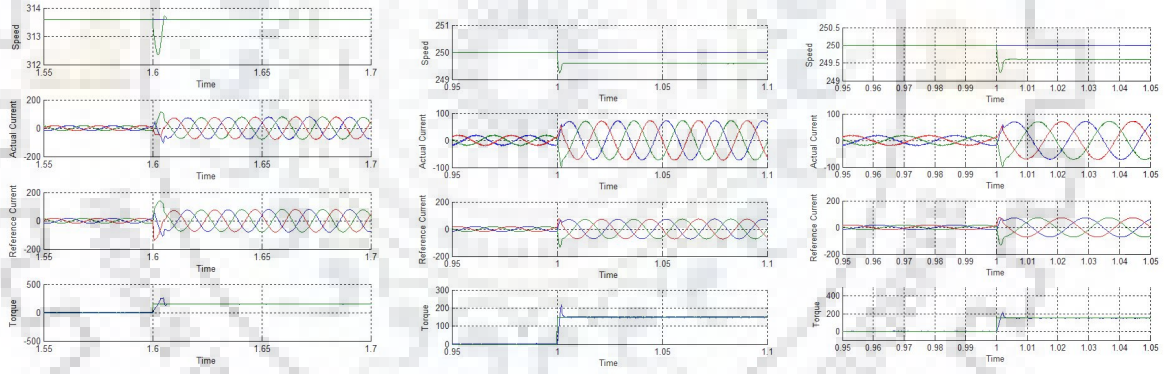

(a) (b) (c)

Fig 3.3 Load application dynamics of VCIMD with (a) PI Controller (b) Fuzzy Logic and (c) Intelligent Controller at constant load when load is applied

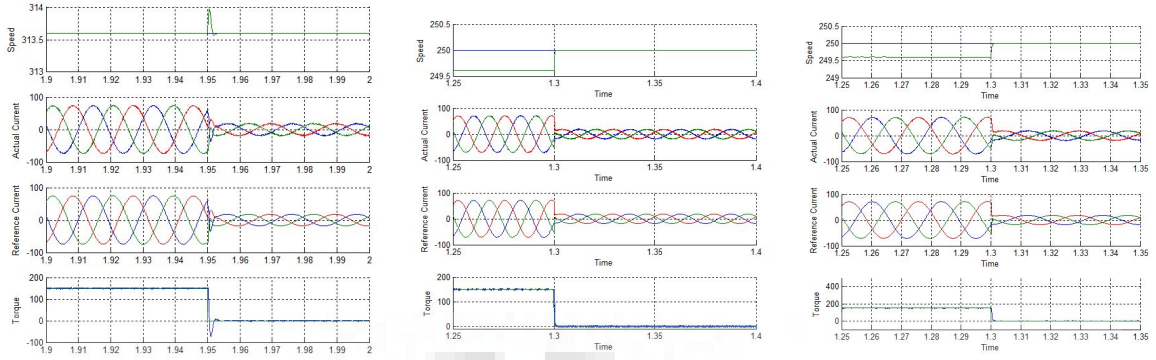

(a) (b) (c)

Fig 3.4 Load removal dynamics of motor VCIMD with (a) PI Controller (b) Fuzzy Logic and (c) Intelligent Controller at constant load when load is applied

LINEAR LOAD

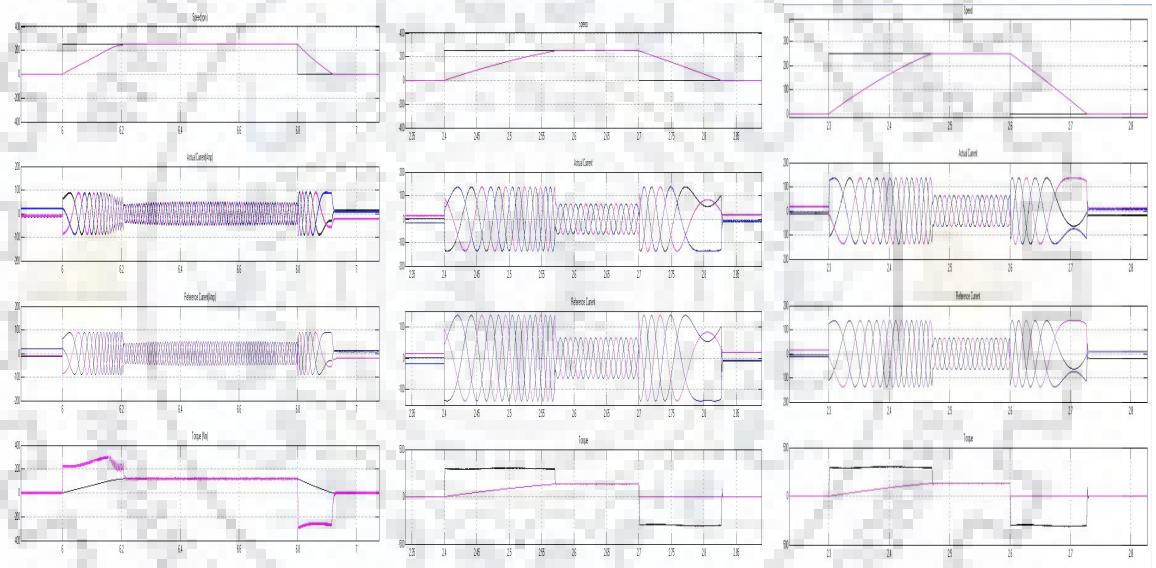

(a) (b) (c)

Fig 3.5 Load perturbation dynamics of VCIMD with (a) PI Controller (b) Fuzzy Logic and (c) Intelligent Controller at constant load when load is applied

QUADRATIC LOAD

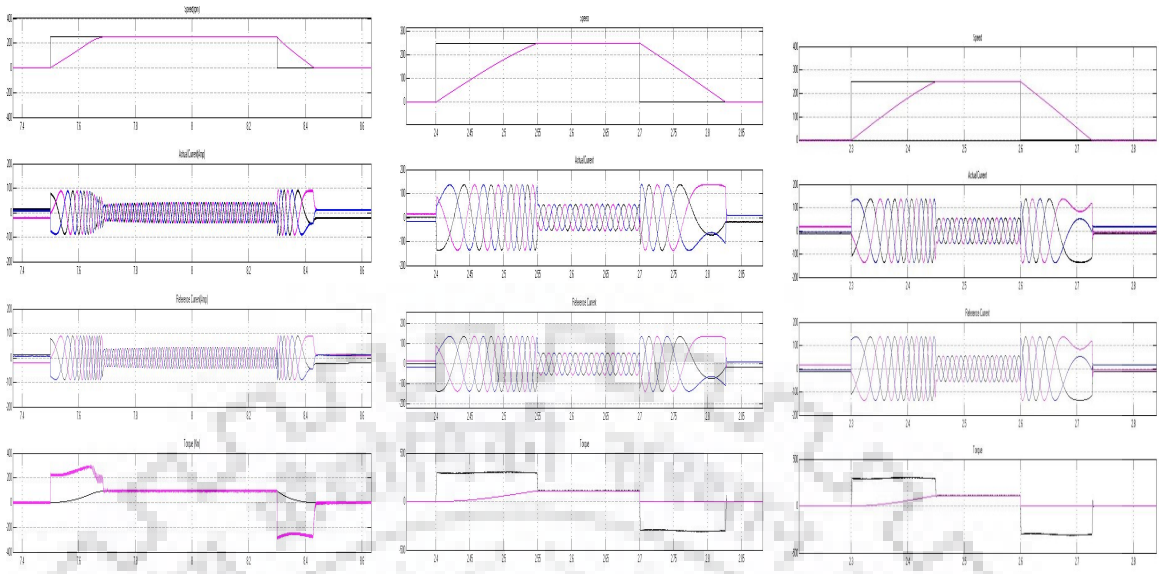

(a) (b) (c)

Fig 3.5 Load perturbation dynamics of VCIMD with (a) PI Controller (b) Fuzzy Logic and (c) Intelligent Controller at constant load when load is applied

3.1.4 COMPARATIVE ANALYSIS

We can see in the table 3.1 and table 3.2 that quick accelaration and fast braking speed is obtained in FL controller. PI have overshoot when step change is applied. FL suffers from the staedy state error. IC can have advantages of both the PI and FL.

Table 3.1 Observations from Various Operating Point

Speed Controller	Starting Time (msec)	Reversal Time (msec)	Bracking Time(msec)	Overshoot in speed at step change
PI	190.0	341	145	0.04
FL	181.0	322	128.0	0
IC	126.0	252	128.5	0.04

Table 3.1 Observations from Load Perturbation

	Constant		Linear		Quadratic	
	Overshoot in speed	Steady state error	Overshoot in sped	Steady state error	Overshoot in sped	Steady state error
PI	0.08	0	0.08	0	0.1	0
FL	0	0.16	0	0.14	0	0.12
IC	0.024	0	0.024	0	0.03	0

3.1.5 CONCLUSION

For simle application PI is used, for intelligent application fuzzy is used. Fuzzy Logic Control suffers with disadvantages such as steady state speed on load. So, the use of intelligent controller which incorporate both features of PI and FL as a function of the speed error for taking the best of both controller.

CHAPTER IV

POWER QUALITY INVESTIGATION OF UNCONTROLLED CONVERTER - INVERTER FED VECTOR COTROLLED INDUCTION MOTOR DRIVE

The detail analysis of vector controlled induction motor drive has been done and described in previous chapters. Dynamic performance of the drive has been observed in various operating conditions and the brief description of the theoretical aspects and the mathematical modelling of vector control induction motor drive have been covered. Since now, AC DC supply was connected to the CC_VSI to feed induction motor operating in vector control mode. In this chapter, the converter inverter arrangement was utilised to feed VCIMD to reduce the cost of system. The AC DC converters are known to have power quality problems such as current harmonics low power factor and heigh THD. The nonlinear loads connected to AC DC Converter inject in the supply, current harmonics in the system and distort the input voltage in the point of common coupling (PCC). This problem create significant disturbances in the supply and the other user which are connected to the same supply will get affected.

4.1 THREE PHASE AC-DC CONVERTER

Three phase converters are used to feed vector control induction motor drive system as shown. The increase number of rectified pulses gives better performance at input side. Various methods have been developed to obtain more number of rectified pulses. These pulses can be obtained in the multiple of 3 and every 3 pulses required one additional three phase bridge converter. Therefore, a number of converters are connected in parallel/series are based on the number of pulses. All these converters are fed by a phase shifting transformer. The harmonic produced by a converter get cancelled by another converter by doing the aapropriate phase shifting at their input supply.

4.2 THREE PHASE UNCONTROLLED AC DC CONVERTER

It has three phase diode bridge rectifier connected to a 3 phase star connected supply voltage with a source impedance Zs. The rectifier is feeding a DC power to VCIMD which is considered as a retrofit system. LC filter is connected between the rectifier and the load. The diode configuration gives the power flow from AC source to inverter feeding VCIMD.

Fig 4.1 shows the matlab model of 3 phase AC DC Converter. A resistance of little value is connected in series with inductor to limit starting current. This resistance is disconnected by a switch after one or two cycles of current. The drive is also connected by a switch which is being controlled by a step function. This function has zero value initially and the switch remains open. after few seconds, when the DC link voltage becomes constant, step signal has one value and the switch is closed. The drive is now connected to the DC voltage. At the same time reference value of speed is given to the speed controller and motor start operating.

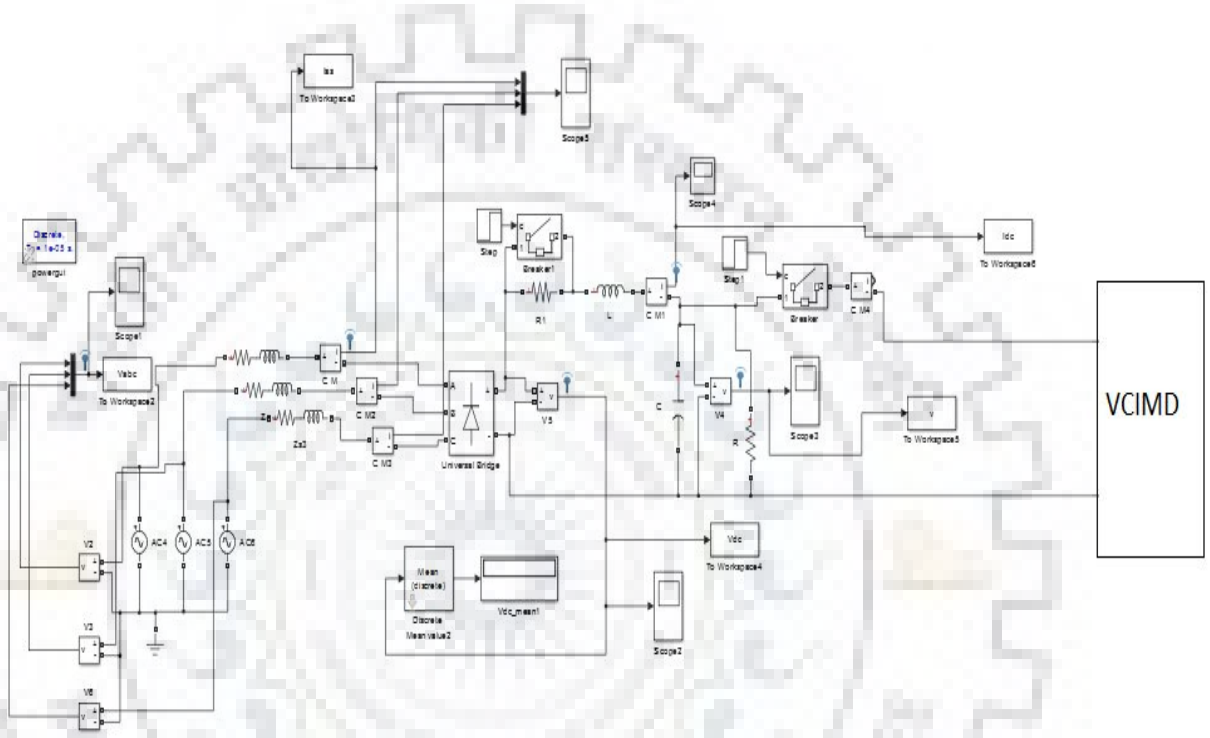

Fig 4.1 MATLAB Model of Three-Phase uncontrolled AC-DC Converter

The performance of VCIMD in starting mode and load perturbation is observed . The machine is operated on full load and the input supply current is observed.

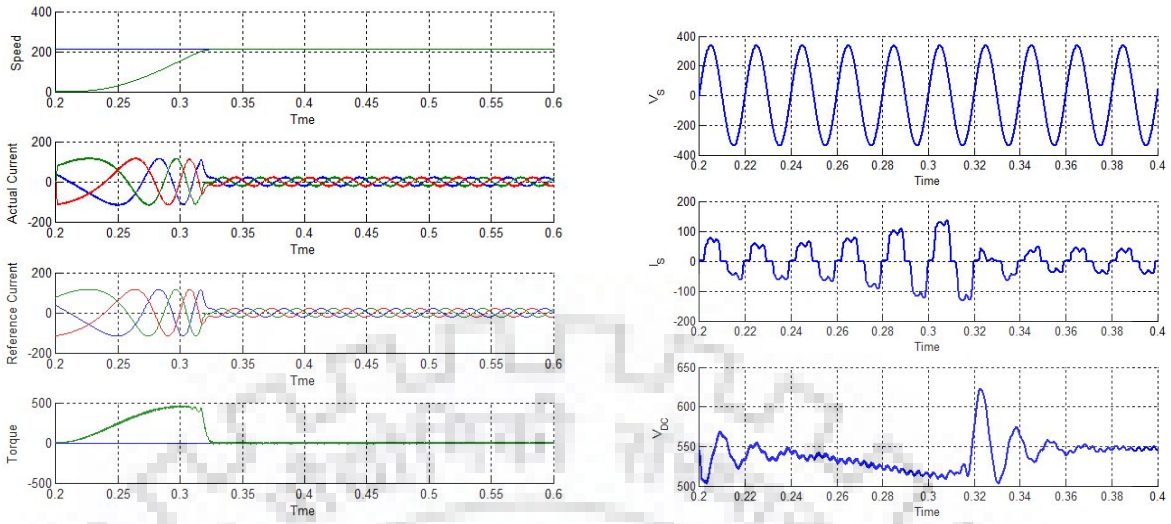

(a) (b)

Fig 4.2 Starting of 3 - Phase uncontrolled AC-DC converter fed VCIMD, (a) Dynamic (b) Source Side

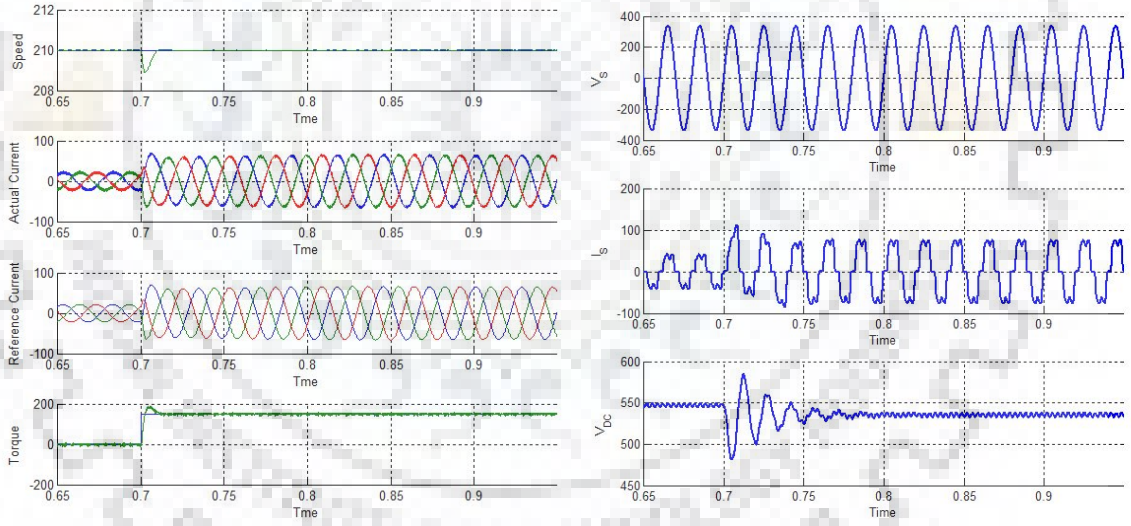

Fig 4.3 Load Application Dynamics of of 3 - Phase uncontrolled AC-DC converter fed VCIMD, (a) Dynamic (b) Source Side

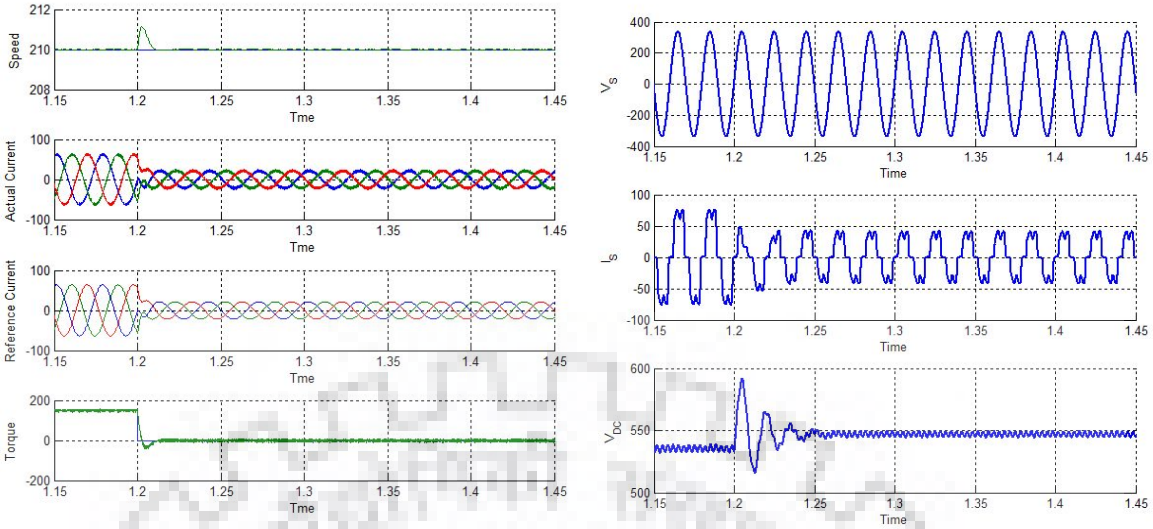

(a) (b)

Fig 4.3 Load Removal Dynamics of of 3 - Phase uncontrolled AC-DC converter fed VCIMD, (a) Dynamic (b) Source Side

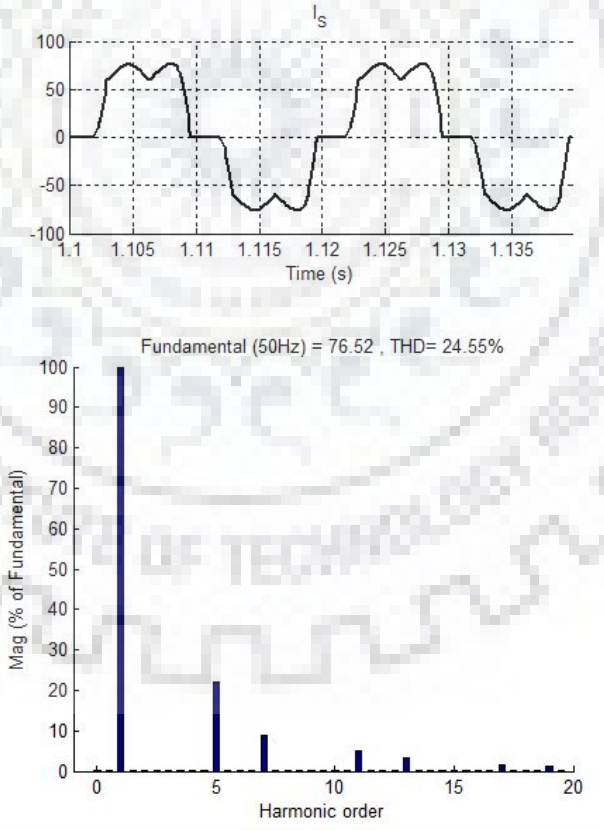

Fig 4.4 THD Analysis of Supply Current of 3 - Phase uncontrolled ac-dc converter fed VCIMD

4.3 MULTIPULSE CONVERTER

To mitigate current harmonics one way is to increase the number of pulses in ac–dc converters. Since a single converter gives six pulses, a multipulse converter is that which gives more than six pulses. For making such a converter, more than one converter is connected in series or in parallel depending on the load requirements. The DC link output is improved using these arrangement and the harmonics are reduced. The converters produce certain harmonics in phase opposition opposition which when added together gets cancelled and thus some harmonics are eliminated on the source side. Certain harmonic gets cancelled by power source itself because these converters produce a particular harmonic in the phase opposition which summed together and cancelled by each other. Various transformer combination can be used to generate more than three phases. The desired phase shift can be obtained by different types of the transformer winding connection such as star, delta, zigzag, fork. polygon etc.
The required phase shift can be calculated as this:

$$\text{Phase Shift} = \frac{360^o}{n}$$

where n denotes the number of pulses required.

In this investigation 12-pulse delta star delta, 12 pulse fork and 24-pulse fork transformers are used to feed VCIMD

4.3.1 DELTA-STAR-DELTA CONNECTED TWELVE PULSE UNCONTROLLED CONVERTER FED VECTOR COTROLLED INDUCTION MOTOR DRIVE

The fig. 4.5 Shows the schematic diagram of twelve pulse converter. It requires a 30^{ö} phase shift. The primary winding is connected in delta and there are two secondary windings one is connected in delta and another in star.
The analysis of such the scheme is given as follows.
On the primary delta side:

$$\begin{aligned} V_{an} &= \frac{\sqrt{2}}{\sqrt{3}} V_L sin(\omega t) \\ V_{bn} &= \frac{\sqrt{2}}{\sqrt{3}} V_L sin(\omega t - 120°) \\ V_{cn} &= \frac{\sqrt{2}}{\sqrt{3}} V_L sin(\omega t + 120°) \end{aligned} \quad (4.1)$$

On the secondary star side:

$$\begin{aligned} V_{ab} &= \frac{\sqrt{2}}{\sqrt{3}} V_L sin(\omega t + 30°) \\ V_{bc} &= \frac{\sqrt{2}}{\sqrt{3}} V_L sin(\omega t - 90°) \\ V_{ca} &= \frac{\sqrt{2}}{\sqrt{3}} V_L sin(\omega t + 150°) \end{aligned} \quad (4.2)$$

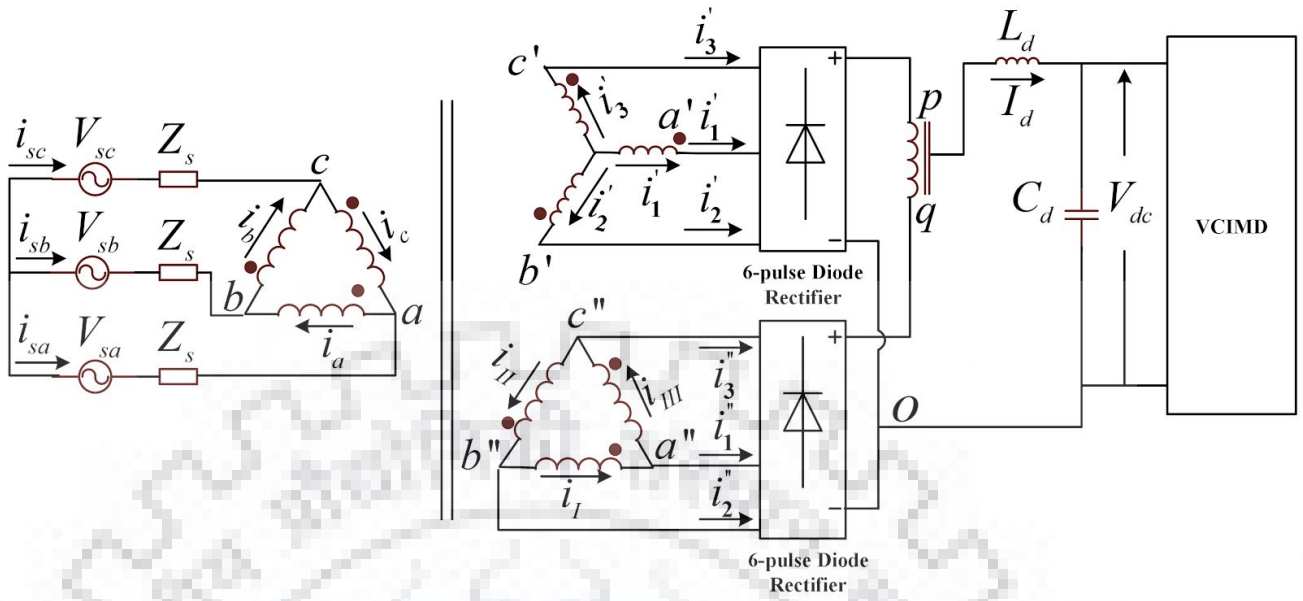

Fig 4.5 Schematic Diagram of Delta/Star-Delta Transformer connected twelve pulse converter

On the secondary delta side:

$$V_{a'b'} = \frac{\sqrt{2}}{\sqrt{3}} V_L sin(\omega t)$$
$$V_{b'c'} = \frac{\sqrt{2}}{\sqrt{3}} V_L sin(\omega t - 120°)$$
$$V_{c'a'} = \frac{\sqrt{2}}{\sqrt{3}} V_L sin(\omega t + 120°) \qquad (4.3)$$

There is a phase difference of 30° between the Primary delta winding and the the Secondary Star connected winding, this is because of the relationship between line and phase voltage of star and delta connection, while there is no such phase difference between the primary and secondary delta connected windings. The fundamental component of supply current and supply voltage will be in the same phase as well. 3 phase voltages of both the windings are 120° displaced from each other. The two secondary windings are connected to two six pulse converters in such a way that they are parallel connected converters and one is supplied by the Delta/Delta and the other is supplied by the Delta/Star connected transformers.

For the interface transformer as shown in fig 4.5 as PQ we obtain between different periods,

1) During 0° to 30 °

$V_{po} = V_{cb}$ $\qquad$ $V_{qo} = V_{c'b'}$

$V_{pq} = V_{cb} - V_{c'b'}$

$= -\sqrt{2}\, V_L sin(\omega t - 90°) + \sqrt{2} V_L sin(\omega t - 120°)$

$= 0.732 V_L sin(wt + 165°)$

At wt = 0° $\qquad$ $V_{pq} = 0.189 V_L$

At wt = 30° $V_{pq} = -0.189V_L$

2) During 30° to 60 °

$V_{po} = V_{ab}$ $V_{qo} = V_{c'b'}$

$V_{pq} = V_{ab} - V_{c'b'}$

$= \sqrt{2}\, V_L \sin(\omega t + 30°) - \sqrt{2}V_L \sin(\omega t - 120°)$

$= 0.732V_L \sin(wt+45°)$

At wt = 30° $V_{pq} = -0.189V_L$

At wt = 60° $V_{pq} = 0.189V_L$

3) During 60° to 90 °

$V_{po} = V_{ab}$ $V_{qo} = V_{a'b'}$

$V_{pq} = V_{ab} - V_{a'b'}$

$= \sqrt{2}\, V_L \sin(\omega t + 30°) - \sqrt{2}V_L \sin(\omega t)$

$= 0.732V_L \sin(wt + 105°)$

At wt = 60° $V_{pq} = 0.189V_L$

At wt = 90° $V_{pq} = -0.189V_L$

3) During 90° to 120 °

$V_{po} = V_{ac}$ $V_{qo} = V_{a'b'}$

$V_{pq} = V_{ac} - V_{a'b'}$

$= -\sqrt{2}\, V_L \sin(\omega t + 150°) - \sqrt{2}V_L \sin(\omega t)$

$= 0.732V_L \sin(wt - 105°)$

At wt = 90° $V_{pq} = -0.189V_L$

At wt = 120° $V_{pq} = 0.189V_L$

4) During 120° to 150 °

$V_{po} = V_{ac}$ $V_{qo} = V_{a'c'}$

$V_{pq} = V_{ac} - V_{a'c'}$

$= -\sqrt{2}\, V_L \sin(\omega t + 150°) + \sqrt{2}V_L \sin(\omega t + 120°)$

$= 0.732V_L \sin(wt + 45°)$

At wt = 120° $V_{pq} = 0.189V_L$

At wt = 150° $V_{pq} = -0.189V_L$

5) During 150° to 180 °

$V_{po} = V_{bc}$ $V_{qo} = V_{a'c'}$

$V_{pq} = V_{bc} - V_{a'c'}$

$= -\sqrt{2}\, V_L \sin(\omega t - 90°) + \sqrt{2}V_L \sin(\omega t + 120°)$

$= 0.732V_L \sin(wt - 165°)$

At wt = 150° $V_{pq} = -0.189V_L$

At wt = 180° $V_{pq} = 0.189V_L$

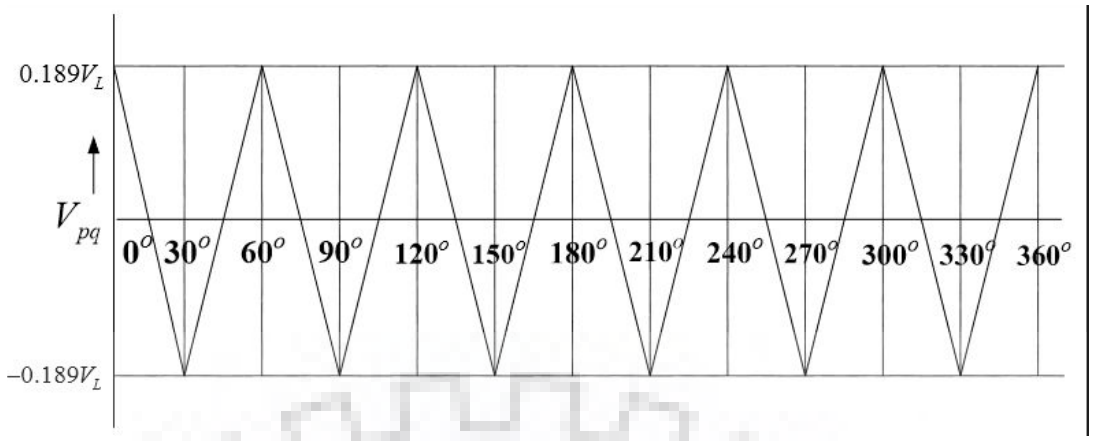

Fig 4.6 Voltage waveform of the interphase transformer winding V_{pq}

Now for 0° to 15° which is the the first quarter cycle = $\int_0^{15°} V_{pq} d\omega t$

$$= \int_0^{15°} 0.732\ V_L \sin(\omega t + 165°) d\omega t$$

$$= 0.732\ V_L [\cos(165°) - \cos(180°)]$$

$$= 0.0249 \times \frac{\pi V_d}{3\sqrt{2}}$$

$$= 0.0180\ V_d \quad (4.4)$$

Area under sine curve of RMS value $V = \int_0^{15°} \sqrt{2}\ V \sin(6\omega t) d\omega t$

$$= \frac{\sqrt{2}}{6} V [\cos(0°) - \cos(90°)]$$

Now, $0.018\ V_d = 0.2357\ V$

$$V = 0.0760\ V_d \quad (4.5)$$

$$KVA_{IR} = VI$$

$$= 0.076\ V_d\ I_d/2$$

$$= \frac{0.076}{2} P_d$$

$$= 3.8\% \text{ of load} \quad (4.6)$$

$$(i_1)_{rms} = \sqrt{\frac{1}{\pi} \int_{\frac{\pi}{6}}^{\frac{5\pi}{6}} \left(\frac{I_d}{2}\right)^2 d\omega t}$$

$$= \sqrt{\frac{I_d^2}{4\pi} \left[\frac{5\pi}{6} - \frac{\pi}{6}\right]}$$

$$= \sqrt{\frac{I_d^2}{4\pi} \cdot \frac{4\pi}{6}}$$

$$= \frac{I_d}{\sqrt{6}} \qquad (4.7)$$

$$(i_1)_{rms} = 0.4082\ I_d$$

$$(i_l)_{rms} = \sqrt{\frac{1}{\pi}\left[\frac{I_d^2}{6} + \frac{I_d^2}{3} + \frac{I_d^2}{6}\right]\frac{\pi}{3}}$$

$$(i_l)_{rms} = 0.2357\ I_d \qquad (4.15)$$

$$(i_1')_{rms} = i_{1P} + i_{IP}$$

$$= \sqrt{\frac{1}{\pi}\left[0.1667^2 + 0.455^2 + 0.622^2\right]\frac{I_d^2}{3}\pi}$$

$$(i_1')_{rms} = 0.4552\ I_d \qquad (4.8)$$

Also,

$$V_d = \frac{3}{\pi} V_{ML}$$

$$= \frac{3\sqrt{2}}{\pi} V_{LL}$$

$$V_L = \frac{\pi}{3\sqrt{2}} V_d \qquad (4.9)$$

$$V_{12} = V_{23} = V_{31} = V_L = \frac{\pi}{3\sqrt{2}} V_d = 0.7405\ V_d \qquad (4.10)$$

$$V_{an} = V_{bn} = V_{cn} = \frac{V_L}{\sqrt{3}} = \frac{\pi}{3\sqrt{6}} V_d = 0.4275\ V_d \qquad (4.11)$$

$$V_{a'b'} = V_{b'c'} = V_{c'a'} = V_L = \frac{\pi}{3\sqrt{2}} V_d = 0.7405\ V_d \qquad (4.12)$$

POWER RATINGS

$$P_d = V_d I_d$$

Primary Delta

$$(KVA_{\triangle})_P = 3\ V_{12} \times (i_1')_{rms}$$

$$= 3 \times 0.7405\ V_d \times 0.4552\ I_d$$

$$(KVA_{\triangle})_P = 1.0112\ P_d \qquad (4.13)$$

Secondary Star

$$(KVA_Y)_S = 3\ V_{an} \times (i_1)_{rms}$$

$$= 3 \times 0.4275\ V_d \times 0.4082\ I_d$$

$$(KVA_Y)_S = 0.5235\ P_d \qquad (4.14)$$

Secondary Delta

$$(KVA_{\triangle})_S = 3\ V_{a'b'} \times (i_l)_{rms}$$

$$= 3 \times 0.7405\ V_d \times 0.2350\ I_d$$

$$(KVA_{\triangle})_S = 0.5236\ P_d \qquad (4.15)$$

Total KVA of the transformer $= \frac{1}{2}\left[(KVA_{\triangle})_P + (KVA_Y)_S + (KVA_{\triangle})_S \right]$

$$= 1.029\ P_d \qquad (4.16)$$

Since, the motor of 30 HP is used, the KVA rating of the tranformer is 1.029 times of the 30 HP, i.e.,

$$= 1.029 \times 30 \times 746 \text{ KVA} = 230.29 \text{ KVA}$$

Also, since the two interphase transformers require 3.8 % of load KVA each, the total KVA requirement of transformers in this scheme comes out to be 400 KVA.

The 3 multi winding transformers are used to realise the Three phase Delta/Star/Delta transformer. Each multi winding transformer has three single phase transformer, one for each primary, secondary star and secondary delta of a single phase. Each of these windings are then connected accordingly. The three winding linear Transformers can also be used to realise the same connection. Modifying the connections of these winding, we can obtain different phase shifts in the multiple of $\pm 30^o$.

Fig 4.8. Shows the simulink model of the Twelve pulse converter.

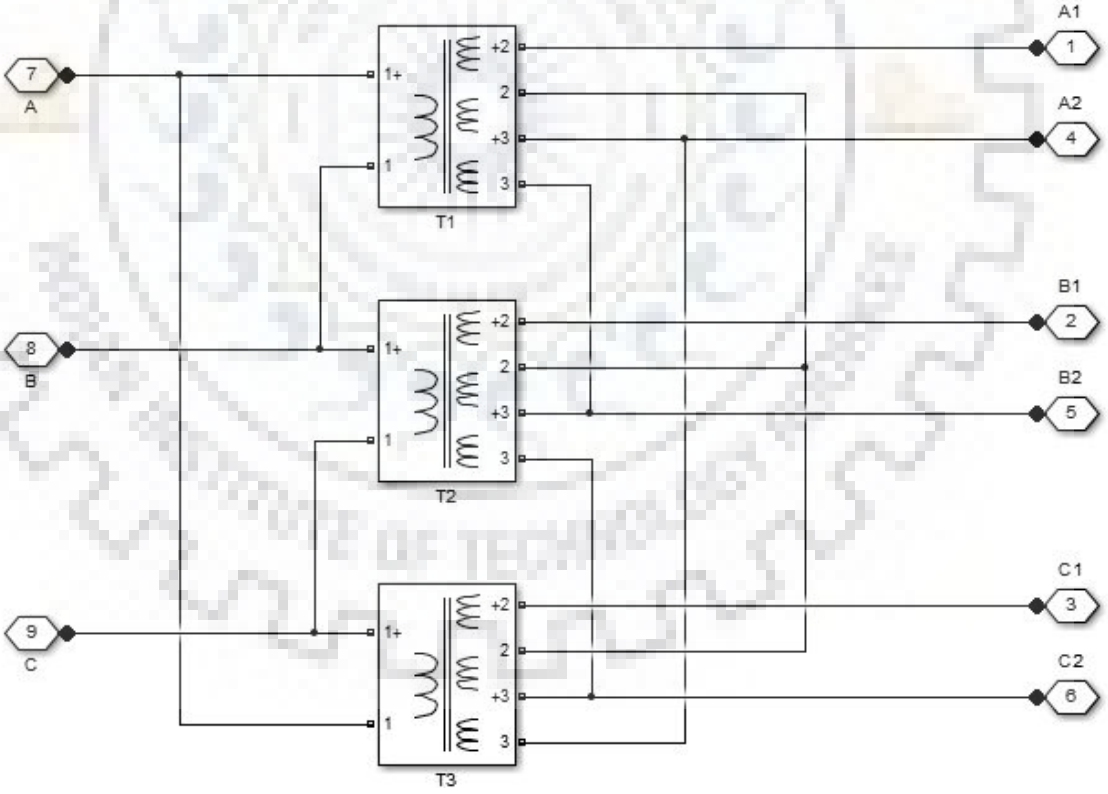

Fig 4.7. MATLAB model of Delta / Star-Delta transformer

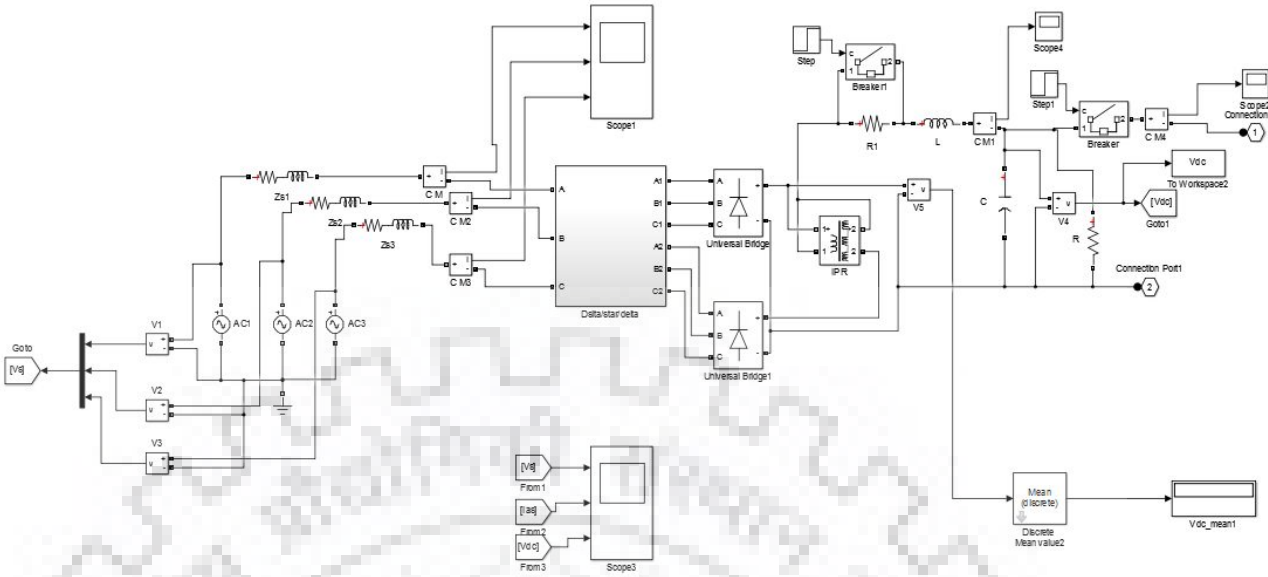

Fig.4.8 MATLAB model of 12 pulse AC-DC converter

As the two converters a connected in parallel the transformation ratio between primary and both secondary is kept 1:1 so that they produce same rms line voltages.

4.3.2. FORK CONNECTED AUTO-TRANSFORMER BASED 12 PULSE UNCONTROLLED CINVERTER FED VECTOR COTROLLED INDUCTION MOTOR DRIVE

It is found that in the 12 pulse converter whic was realised using two 6 - pulse converter connected to the Delta/ Star Delta transformer, as been investigated in section 4. The 12 pulse converter eliminates the fifth and seventh harmonics from the supply side. The KVA rating is found to be around 1.03 P_d (pu) in equation (4.16).

Another polyphase transformer arrangement can be utilised to obtain 12 pulse throw connection with two converters. Such as the topology is shown in Fig 4.9 which is used for a 12-pulse AC-DC converter.

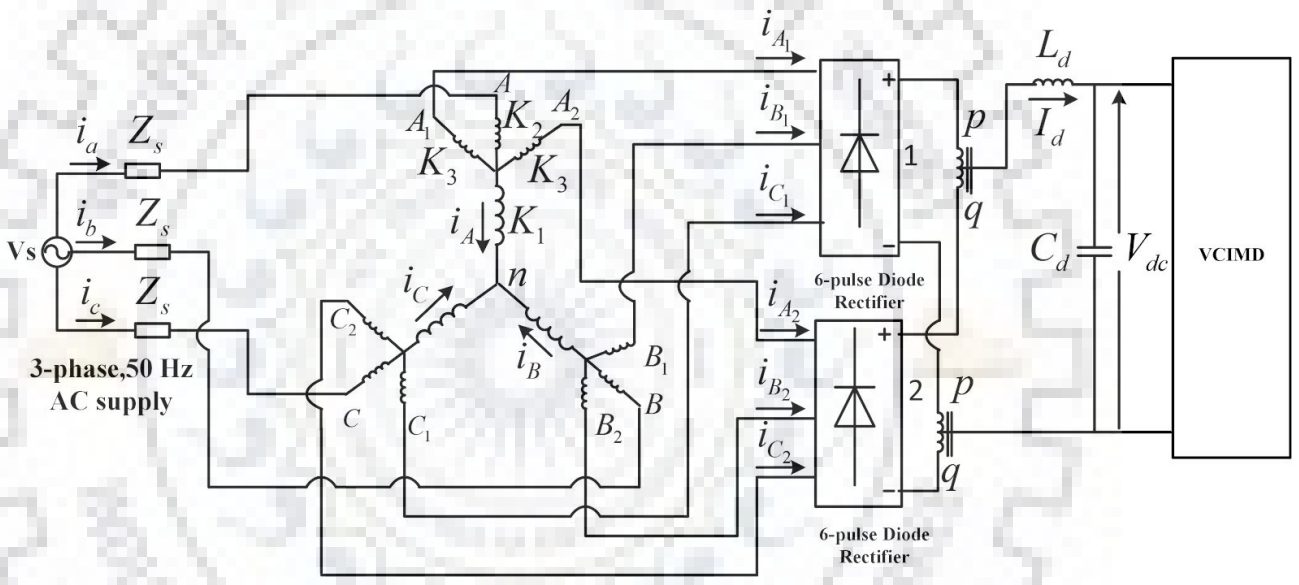

Fig 4.9. 12 pulse AC-DC converter based on fork transformer topology

This topology uses an auto connected fork-transformer. It is connected to two six-pulse diode bridge converters on the DC side through inter-phase transformers. As it is an autotransformer the KVA transferred through magnetic coupling is only a part of total KVA. For the same KVA rating, the size of this transformer can be smaller than the isolation transformers of Delta/Star-Delta type. It can also be more light and less costly than the isolation transformer.

The Fork transformer can be investigated as such,

For producing twelve pulse rectification, the following requirements have to be met,

a) The transformer should produce two sets of balanced line voltages, which must be out of phase with each other by either ±15° or ±30° .

b) The voltage magnitude should be equal to produce symmetrical pulses so thatt th ripple in output voltage is reduced.

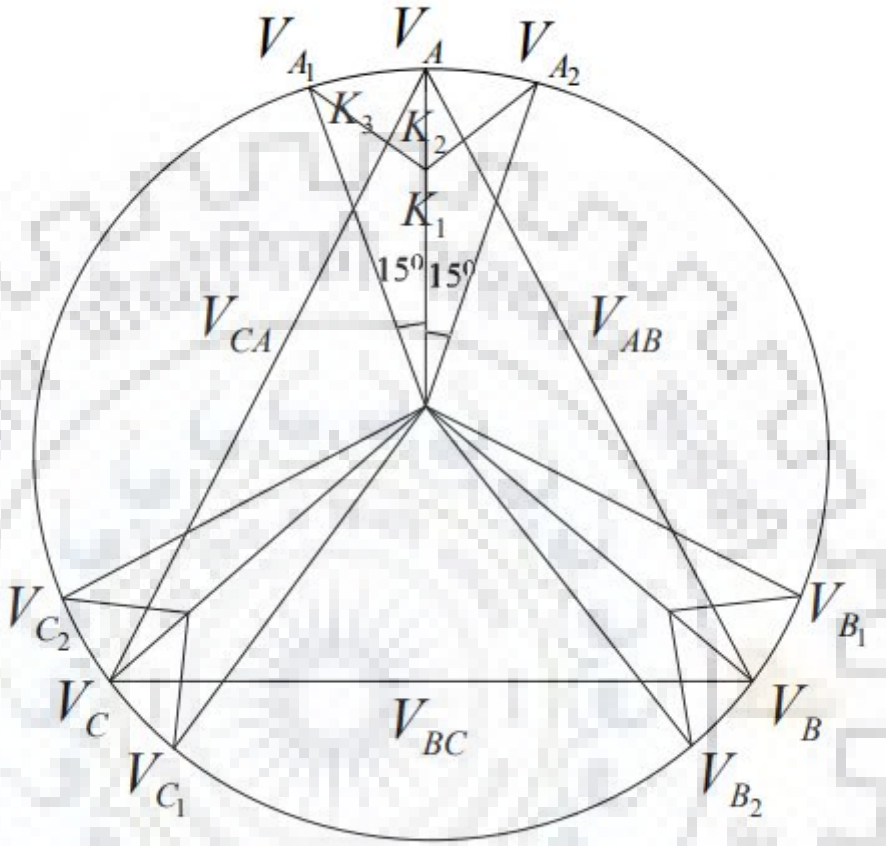

Fig.4.10. Phasor diagram of the fork transformer

The phasor diagram of the fork transformer is shown in fig. 4.10. It shows the relationship among various phases. From the phasor diagram it is shown that here, 15^0 phase shift is used to fulfill condition (a).

Two sets of line Voltages from the supply voltage is produced. The number of turns can be calculated as follows:

Let the input phase voltage is V_A and the set of three phase voltages connected to each converter be V_{A1}, V_{Bl}, V_{C1}; and V_{A2}, V_{B2},V_{C2}; connected to the converters 1 and 2 respectively as shown in fig 4.9.

$V_A = V_{ac}/3;$

$V_A = V_S\angle 0°$ $\quad V_B = V_S \angle -120°$ $\quad V_C = V_S\angle 120°$

$V_{A1} = V_S\angle 15°$ $\quad V_{B1} = V_S\angle -105°$ $\quad V_{C1} = V_S\angle 135°$

$V_{A2} = V_S\angle -15°$ $\quad V_{B2} = V_S\angle -135°$ $\quad V_{C2} = V_S\angle 105°$

(4.17)

If the secondary voltage are known, voltages of converters can be shown in these ways. The secondary winding voltages can be shown as,

$$V_A = K_1 V_A + K_2 V_A$$

$$K_1 + K_2 = 1$$

$$V_{A1} = K_1 V_S \angle 0° - K_3 V_S \angle -120°$$

$$V_S \angle 15° = K_1 V_S \angle 0° - K_3 V_S \angle -120°$$

We obtain solving these equations,

$$K_1 = 0.8165 \qquad K_2 = 0.1835 \qquad K_3 = 0.2988$$

(4.18)

$$\Rightarrow V_{A1} = K_1 V_A - K_3 V_B = 0.8165 V_A - 0.2988 V_B$$
$$\Rightarrow V_{A2} = K_1 V_A - K_3 V_C = 0.8165 V_A - 0.2988 V_C$$
$$\Rightarrow V_{B1} = K_1 V_B - K_3 V_C = 0.8165 V_B - 0.2988 V_C$$
$$\Rightarrow V_{B2} = K_1 V_B - K_3 V_A = 0.8165 V_B - 0.2988 V_A$$
$$\Rightarrow V_{C1} = K_1 V_C - K_3 V_A = 0.8165 V_C - 0.2988 V_A$$
$$\Rightarrow V_{C2} = K_1 V_C - K_3 V_B = 0.8165 V_C - 0.2988 V_B$$

(4.27)

POWER RATINGS

$$P_d = V_d I_d$$

$$V_d = \frac{3}{\pi} V_{ML}$$

$$= \frac{3\sqrt{2}}{\pi} V_{LL}$$

(4.19)

VOLTAGE RATINGS

$$V_{zig} = K_3 V_S = 0.2988 V_S$$
$$V_{ph} = K_1 V_S = 0.8165 V_S$$
$$V_{in} = K_2 V_S = 0.1836 V_S$$

(4.20)

CURRENT RATINGS

$$i_a = i_{A1} + i_{A2} + i_A$$
$$i_b = i_{B1} + i_{B2} + i_B$$
$$i_c = i_{C1} + i_{C2} + i_C$$

(4.21)

In phase A

$$i_A = - \left[\frac{K_2 i_a + K_1 i_A K_3 i_{C1} K_3 i_{B2}}{K_1 + K_2} \right]$$

(4.22)

Similarly in phase C and in phase B.

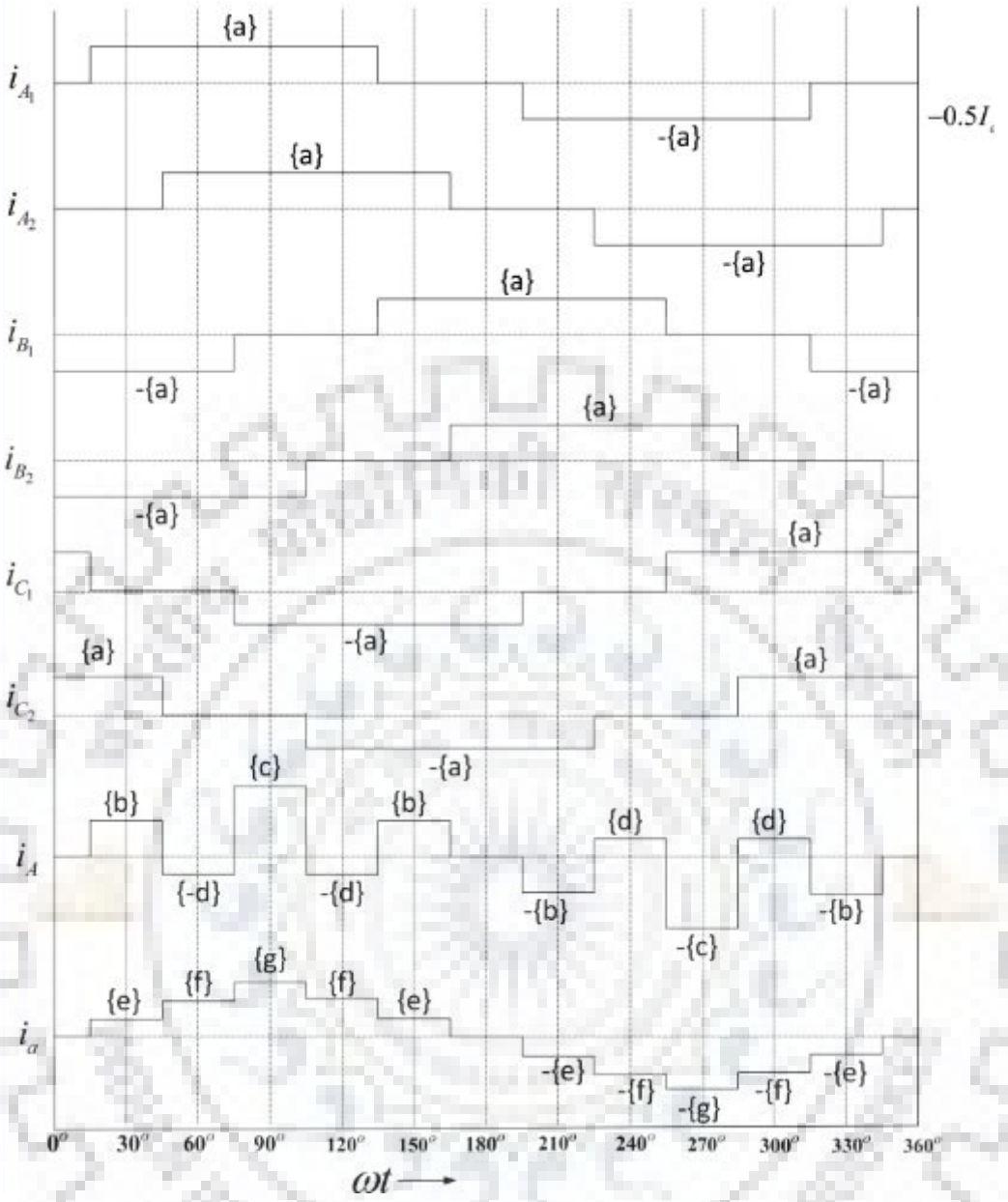

Fig. 4.11 Current waveform in diffenrent windings of fork transformer on constant load

Values {a} through {g} are:

{a} = v0.5 I_d; {b} =v 0.05765 I_d; {c} = 0.1153I_d; {d} = 0.0341I_d;

{e} = 0.3576I_d; {f} = 0.9659I_d; {g} = 1.1153I_d.

Calculating these on constant current load whose result is as shown in fig.4.11. , we get the following values,

$$(i_A)_{rms} = 0.0609\ I_d$$
$$(i_a)_{rms} = 0.7886\ I_d$$
$$(i_{A1})_{rms} = 0.4082\ I_d \qquad (4.23)$$

From equations (4.19), (4.20) and (4.23), we get,

$I_{zig} = (i_{A1})_{rms} = 0.4082\ I_d$ $\quad V_{zig} = K_3 V_S = 0.2988 V_S$

$I_{ph} = (i_a)_{rms} = 0.7886\ I_d$ $\quad V_{ph} = K_1 V_S = 0.8165 V_S$

$I_{in} = (i_a)_{rms} = 0.7886\ I_d$ $\quad V_{in} = K_2 V_S = 0.1836 V_S$

And,

$$KVA_{zig} = I_{zig} V_{zig} = 0.052 P_d$$
$$KVA_{ph} = I_{ph} V_{ph} = 0.213 P_d$$
$$KVA_{in} = I_{in} V_{in} = 0.618 P_d$$
$$KVA\ total = \frac{1}{2}[6 \times KVA_{zig} + 3 \times KVA_{ph} + 3 \times KVA_{in}]$$
$$= 0.28095\ P_d \qquad (4.24)$$

This mean, it requires 28.095 % of load for transformer, which is lower than that of isolation transformer, compare (4.24).

INTERPHASE REACTOR RATING

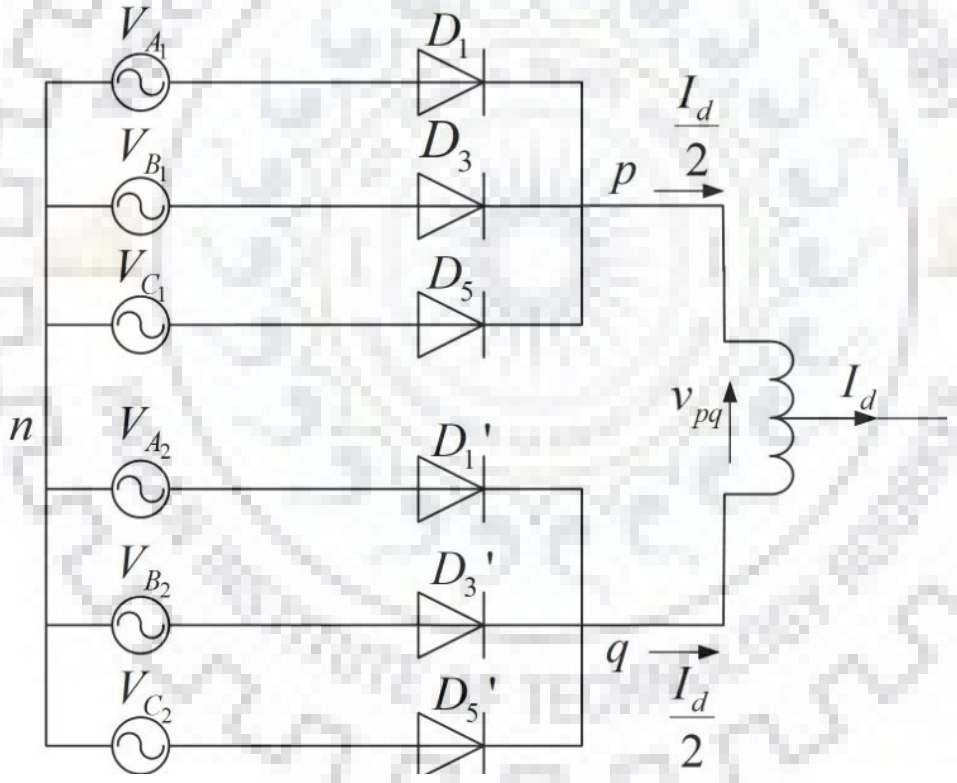

Fig 4.12. Interphase Reactor

We consider the following equations

$V_{A1} = V_S \sin(\omega t + 15°)$ $\quad V_{B1} = V_S \sin(\omega t - 105°)$ $\quad V_{C1} = V_S \sin(\omega t + 135°)$

$V_{A2} = V_S \sin(\omega t - 15°)$ $\quad V_{B2} = V_S \sin(\omega t - 135°)$ $\quad V_{C2} = V_S \sin(\omega t + 105°)$

1) During 0 ° to 15 °

$$V_{po} = V_{C1} \qquad V_{qo} = V_{C2}$$

$$V_{pq} = V_{C1} - V_{C2}$$

$$= V_M[\sin(\omega t + 135°) - \sin(\omega t - 105°)$$

$$= 0.5179V_M\sin(wt-150°)$$

At wt = 0° $V_{pq} = -0.2588V_M$

At wt = 15° $V_{pq} = -0.3669V_M$

2) During 15° to 45 °

$$V_{po} = V_{A1} \qquad V_{qo} = V_{C2}$$

$$V_{pq} = V_{A1} - V_{C2}$$

$$= V_M[\sin(\omega t + 15°) - \sin(\omega t - 105°)$$

$$= 1.4142V_M\sin(wt-30°)$$

At wt = 15° $V_{pq} = -0.3659V_M$

At wt = 45° $V_{pq} = 0.3669V_M$

3) During 45° to 75 °

$$V_{po} = V_{A1} \qquad V_{qo} = V_{A2}$$

$$V_{pq} = V_{A1} - V_{C2}$$

$$= V_M[\sin(\omega t + 15°) - \sin(\omega t - 15°)$$

$$= 0.5176V_M\sin(wt+90°)$$

At wt = 45° $V_{pq} = 0.3659V_M$

At wt = 75° $V_{pq} = 0.1339V_M$

4) During 75° to 105 °

$$V_{po} = V_{A1} \qquad V_{qo} = V_{A2}$$

$$V_{pq} = V_{A1} - V_{C2}$$

$$= V_M[\sin(\omega t + 15°) - \sin(\omega t - 15°)$$

$$= 0.5176V_M\sin(wt+90°)$$

At wt = 75° $V_{pq} = 0.3659V_M$

At wt = 105° $V_{pq} = -0.1339V_M$

5) During 105° to 135 °

$$V_{po} = V_{A1} \qquad V_{qo} = V_{A2}$$

$$V_{pq} = V_{A1} - V_{C2}$$

$$= V_M[\sin(\omega t + 15°) - \sin(\omega t - 15°)$$

$$= 0.5176V_M\sin(wt+90°)$$

At wt = 105° $V_{pq} = -0.1339V_M$

At wt = 1355° $V_{pq} = 3659V_M$

6) During 135° to 165 °

$$V_{po} = V_{B1} \qquad V_{qo} = V_{A2}$$

$$V_{pq} = V_{B1} - V_{A2}$$
$$= V_M[\sin(\omega t + 135°) - \sin(\omega t - 15°)$$
$$= 1.414V_M\sin(wt-150°)$$

At wt = 135° $V_{pq} = -0.3659V_M$

At wt = 165° $V_{pq} = 0.3659V_M$

7) During 165° to 195 °

$$V_{po} = V_{B1} \qquad V_{qo} = V_{B2}$$
$$V_{pq} = V_{B1} - V_{B2}$$
$$= V_M[\sin(\omega t + 105°) - \sin(\omega t - 135°)$$
$$= 0.5176V_M\sin(wt-30°)$$

At wt = 165° $V_{pq} = 0.3659V_M$

At wt = 195° $V_{pq} = 0.13396V_M$

8) During 195° to 225 °

$$V_{po} = V_{B1} \qquad V_{qo} = V_{B2}$$
$$V_{pq} = V_{B1} - V_{B2}$$
$$= V_M[\sin(\omega t + 105°) - \sin(\omega t - 135°)]$$
$$= 0.5176V_M\sin(wt-30°)$$

At wt = 195° $V_{pq} = 0.13396V_M$

At wt = 225° $V_{pq} = -0.13396V_M$

9) During 225° to 255 °

$$V_{po} = V_{C1} \qquad V_{qo} = V_{B2}$$
$$V_{pq} = V_{C1} - V_{B2}$$
$$= V_M[\sin(\omega t + 135°) - \sin(\omega t - 135°)]$$
$$== 0.5176V_M\sin(wt-30°)$$

At wt = 225° $V_{pq} = -0.13396V_M$

At wt = 255° $V_{pq} = -0.3659V_M$

10) During 225° to 255 °

$$V_{po} = V_{C1} \qquad V_{qo} = V_{B2}$$
$$V_{pq} = V_{C1} - V_{B2}$$
$$= V_M[\sin(\omega t + 135°) - \sin(\omega t - 135°)]$$
$$= 1.414V_M\sin(wt+90°)$$

At wt = 225° $V_{pq} = -0.3659V_M$

At wt = 255° $V_{pq} = 0.3659V_M$

11) During 255° to 285 °

$$V_{po} = V_{C1} \qquad V_{qo} = V_{C2}$$
$$V_{pq} = V_{C1} - V_{C2}$$
$$= V_M[\sin(\omega t\ 135°) - \sin(\omega t - 105°)$$

$= 0.5179V_M \sin(\omega t - 150°)$

At wt = 255° $V_{pq} = 0.3659V_M$

At wt = 2885° $V_{pq} = 0.13396V_M$

12) During 285° to 345 °

$V_{po} = V_{C1}$ $V_{qo} = V_{C2}$

$V_{pq} = V_{C1} - V_{C2}$

$= V_M[\sin(\omega t\ 135°) - \sin(\omega t - 105°)$

$= 0.5179V_M \sin(\omega t - 150°)$

At wt = 255° $V_{pq} = 0.13396V_M$

At wt = 345° $V_{pq} = -0.13396V_M$

13) During 345° to 360 °

$V_{po} = V_{C1}$ $V_{qo} = V_{C2}$

$V_{pq} = V_{C1} - V_{C2}$

$= V_M[\sin(\omega t\ 135°) - \sin(\omega t - 105°)$

$= 0.5179V_M \sin(\omega t - 150°)$

At wt = 345° $V_{pq} = -0.13396V_M$

At wt = 360° $V_{pq} = -0.2588V_M$

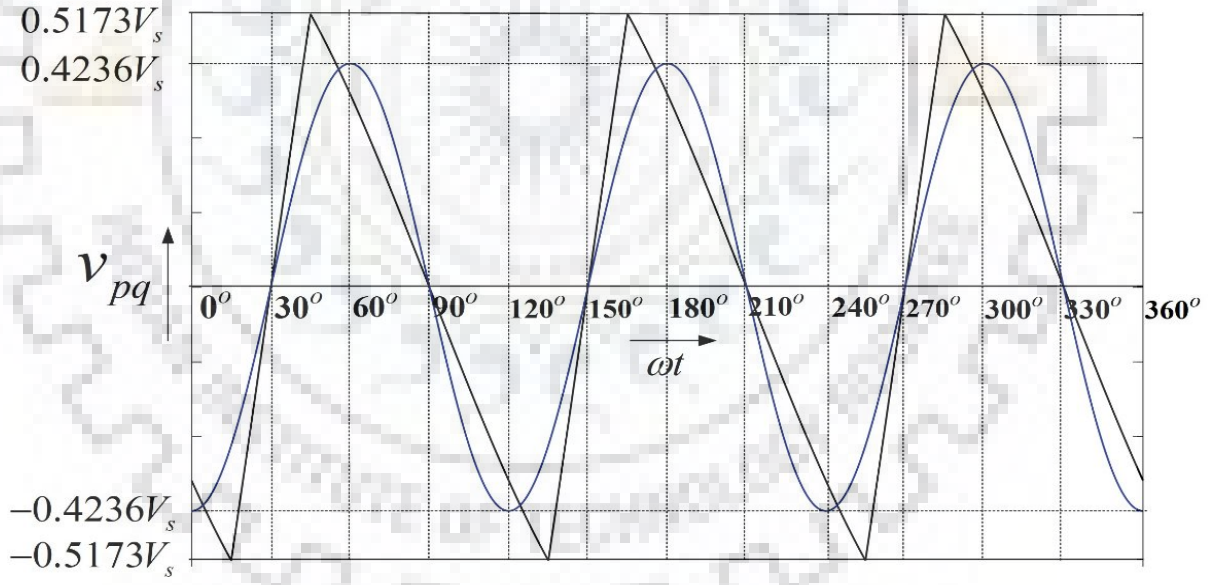

Fig 4.13. The voltage vaweform in the interface winding

Now for 0° to 15° which is the the first quarter cycle = $\int_0^{15°} V_{pq} d\omega t$

$= \int_0^{15°} 0.5176\ V_M \sin(\omega t - 160°) d\omega t$

$= 0.5176\ V_L [\cos(-150°) - \cos(-135°)]$

$= -0.0822V_M$

$$= 0.0822 \times \frac{\pi V_d}{3\sqrt{6}}$$

$$= 0.049\ V_d \qquad (4.25)$$

Area under sine curve of RMS value $V = \int_0^{15°} \sqrt{2}\ V \sin(6\omega t) d\omega t$

$$= \frac{\sqrt{2}}{6} V\ [\cos(0°) - \cos(90°)]$$

Now, $0.0498\ V_d = 0.2357\ V$

$V = 0.207 V_d$

From equations ….. We can get,

$$KVA_{IR} = VI$$

$$= 0.207 V_d \times I_d/2$$

$$= 0.1035\ P_d$$

Which means that the interphase transformer, here two such transformers required, will need 10.35 % of load KVA. Therefore the total KVA rating of Fork transformer will be 48.795% of load, which is less than that required in isolated Delta/ Star-Delta transformer.

The MATLAB model of 12 pulse fork converter is shown in fig. 4.14
It is realised through multi winding transformer with appropriate values.

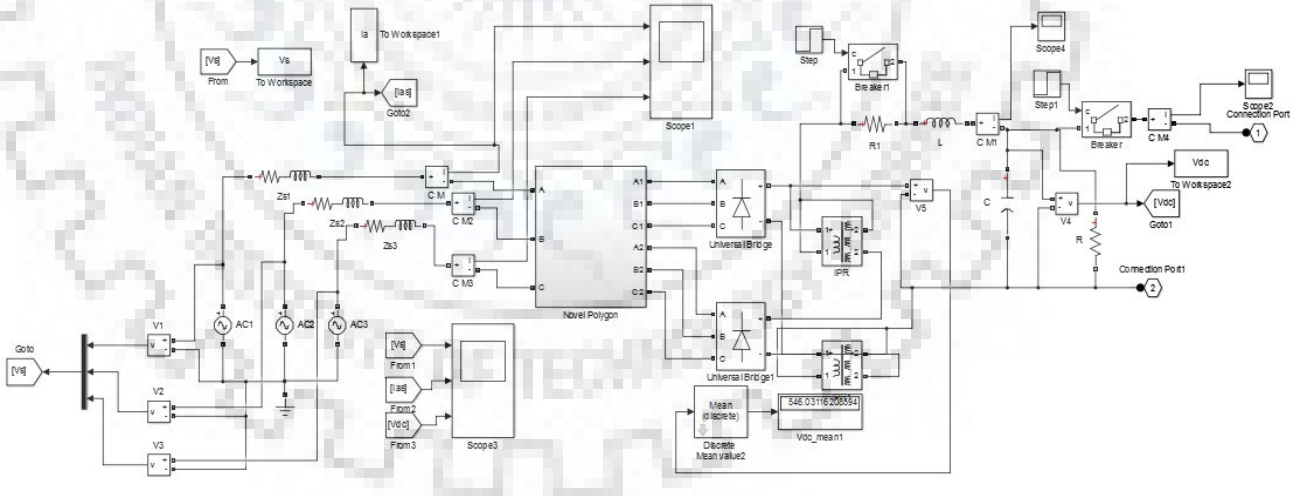

Fig 4.14 MATLAB model of 12 pulse AC-DC converter

Each multi winding transformer has single phase transformer, there are 4 windings on each transformer . Each of these windings are then connected accordingly.

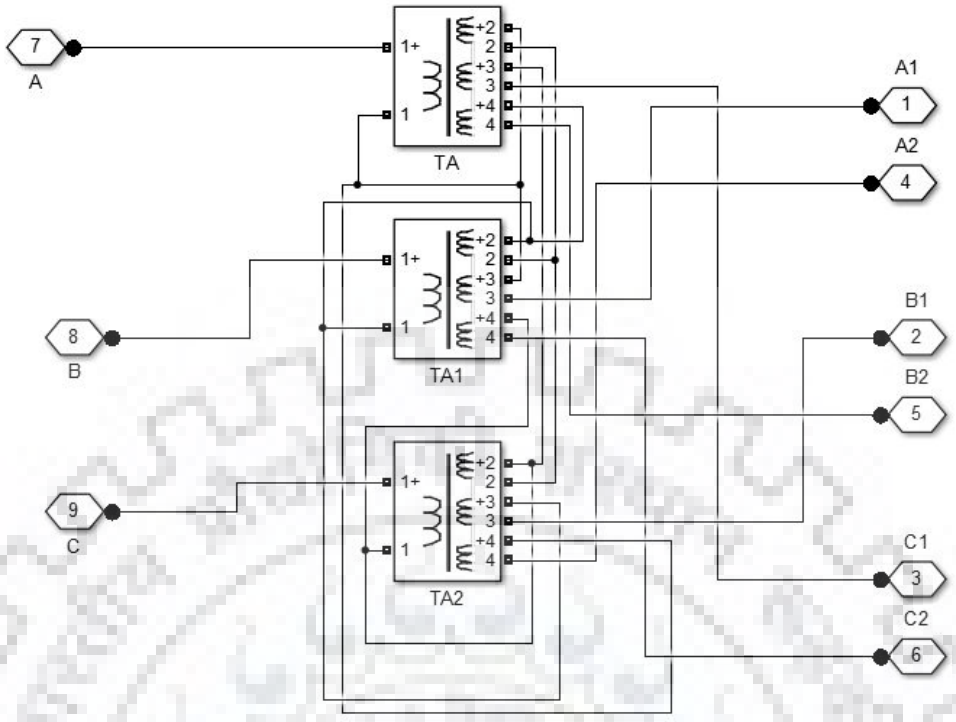

Fig 4.15 MATLAB model of fork auto transformer

4.3.3. FORK CONNECTED AUTO-TRANSFORMER BASED 24 PULSE CINVERTER FED VECTOR COTROLLED INDUCTION MOTOR DRIVE

Another polyphase transformer arrangement can be utilised to obtain 24 pulse throw connection with two converters. Such as the topology is shown in Fig 4.16 which is used for a 24-pulse AC-DC converter

Some applications have very high power quality requirenments. Although by using tuned passive filters the harmonics in input current and output voltage of conventional 12-pulse uncontrolled rectifiers can be reduced, these filters arelossy and bulky. In such a situation, it is a need to use higher pulse AC-DC converter system. And to meet the standard requirements of IEEE-519 for AC-DC conversion it is suggested that higher pulse AC-DC converter must be used. A 24-pulse AC-DC converter is designed using fork connected auto-transformer.

This topology also uses an auto connected fork-transformer. It is connected to four six-pulse diode bridge converters on the DC side through inter-phase transformers. The fork autotransformer will produce four sets of three phase voltages. The unlike phases of secondary windings of different single-phase transformers are interconnected to form fork arrangement. The Converters are connected in parallel producing 24-pulse AC-DC converter configuration.

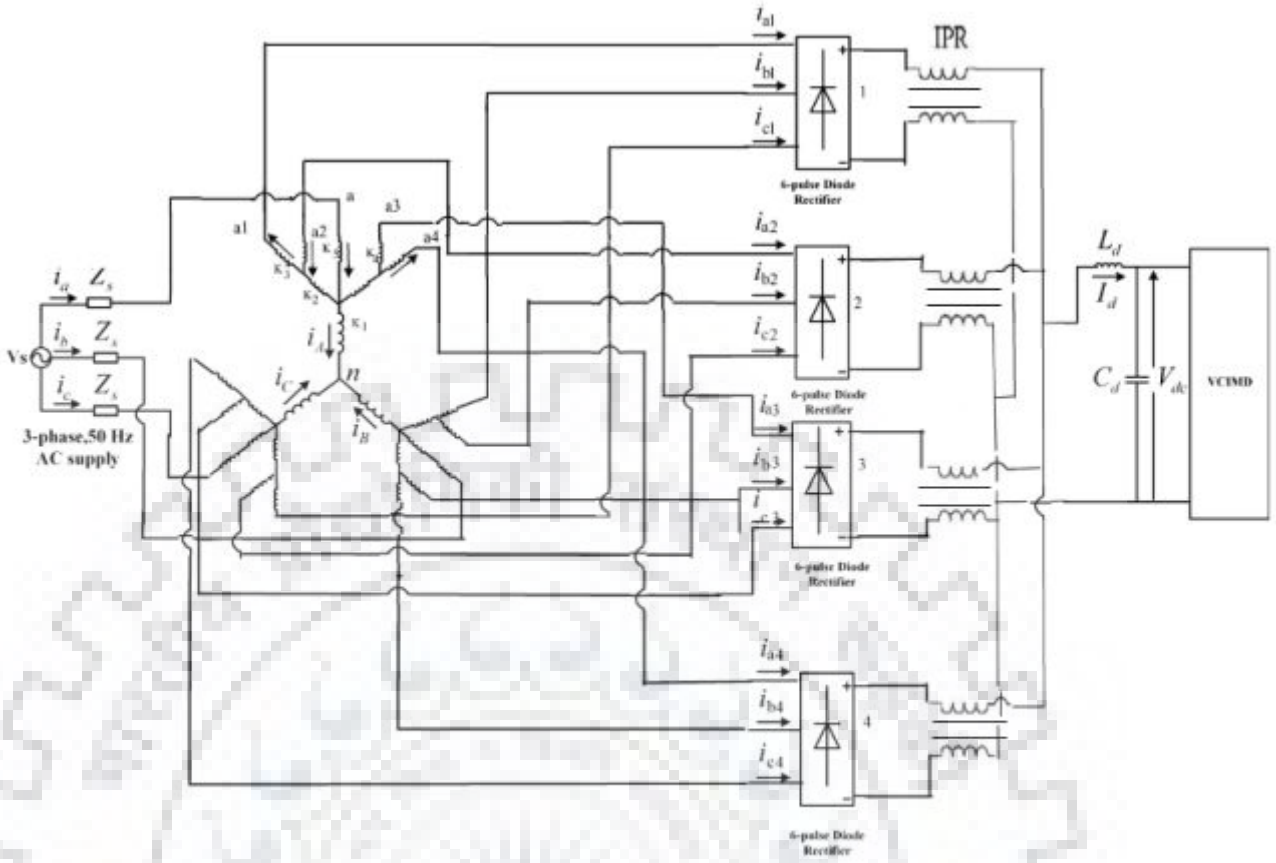

Fig 4.16. A 24 pulse AC-DC converter based on fork transformer topology

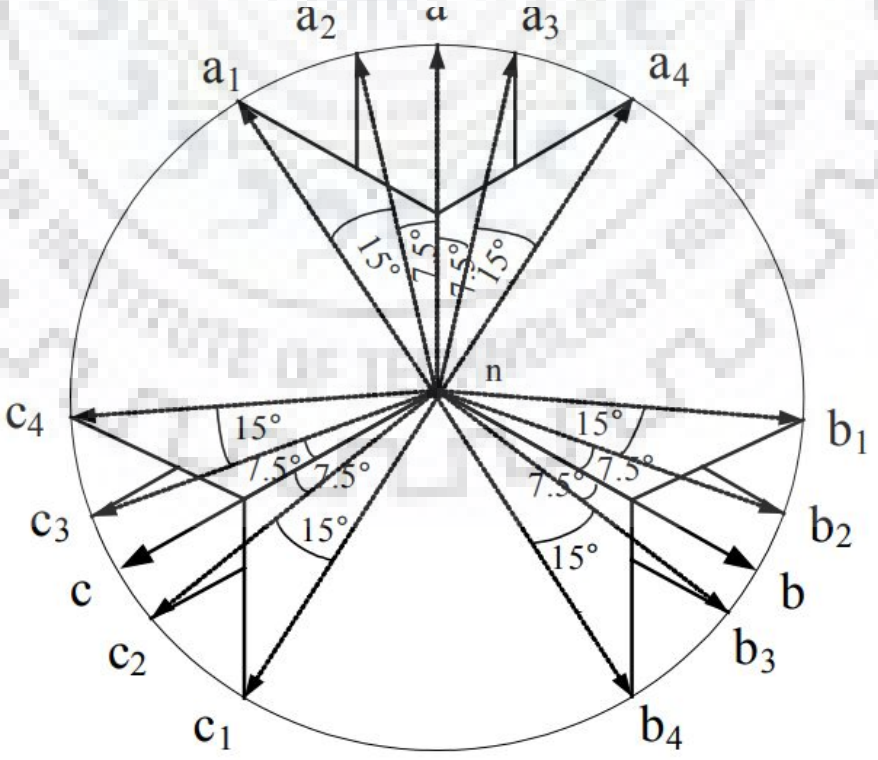

Fig.4.17. Phasor diagram of the fork transformer

The Fork transformer can be investigated as such,

The phasor diagram of the fork transformer is shown in fig. 4.17 . It shows the relationship between various phases. The winding scheme of fork autotransformer for 24- pulse AC-DC conversion is shown in Fig. 4.16.

Four sets of line Voltages from the supply volatage is produced which are are displaced at an angle of 15°, two sets of which line Voltages from the are displaced from the input phase voltage at an angle of ±7.5° and two at an angle of ±22.5°. The number of turns can be calculated as follows:

Let the input phase voltage is V_A and the set of three phase voltages connected to each converter be V_{A1}, V_{Bl}, V_{C1}; V_{A2}, V_{B2},V_{C2}; V_{A3}, V_{B3}, V_{C3}; and V_{A4}, V_{B4},V_{C4}; connected to the converters 1 to 4 respectively as shown in fig 4.17.

$$V_A = V_{ac}/3;$$

$$V_A = V_S\angle 0° \qquad V_B = V_S\angle -120° \qquad V_C = V_S\angle 120°$$

$$V_{A1} = V_S\angle 22.55° \qquad V_{B1} = V_S\angle -97.5° \qquad V_{C1} = V_S\angle -217.5°$$

$$V_{A2} = V_S\angle 7.5° \qquad V_{B2} = V_S\angle -112.5° \qquad V_{C2} = V_S\angle -232.5°$$

$$V_{A3} = V_S\angle -7.5° \qquad V_{B3} = V_S\angle -127.5° \qquad V_{C3} = V_S\angle -247.5°$$

$$V_{A4} = V_S\angle -22.55° \qquad V_{B4} = V_S\angle -142.5° \qquad V_{C4} = V_S\angle -262.5° \qquad (4.26)$$

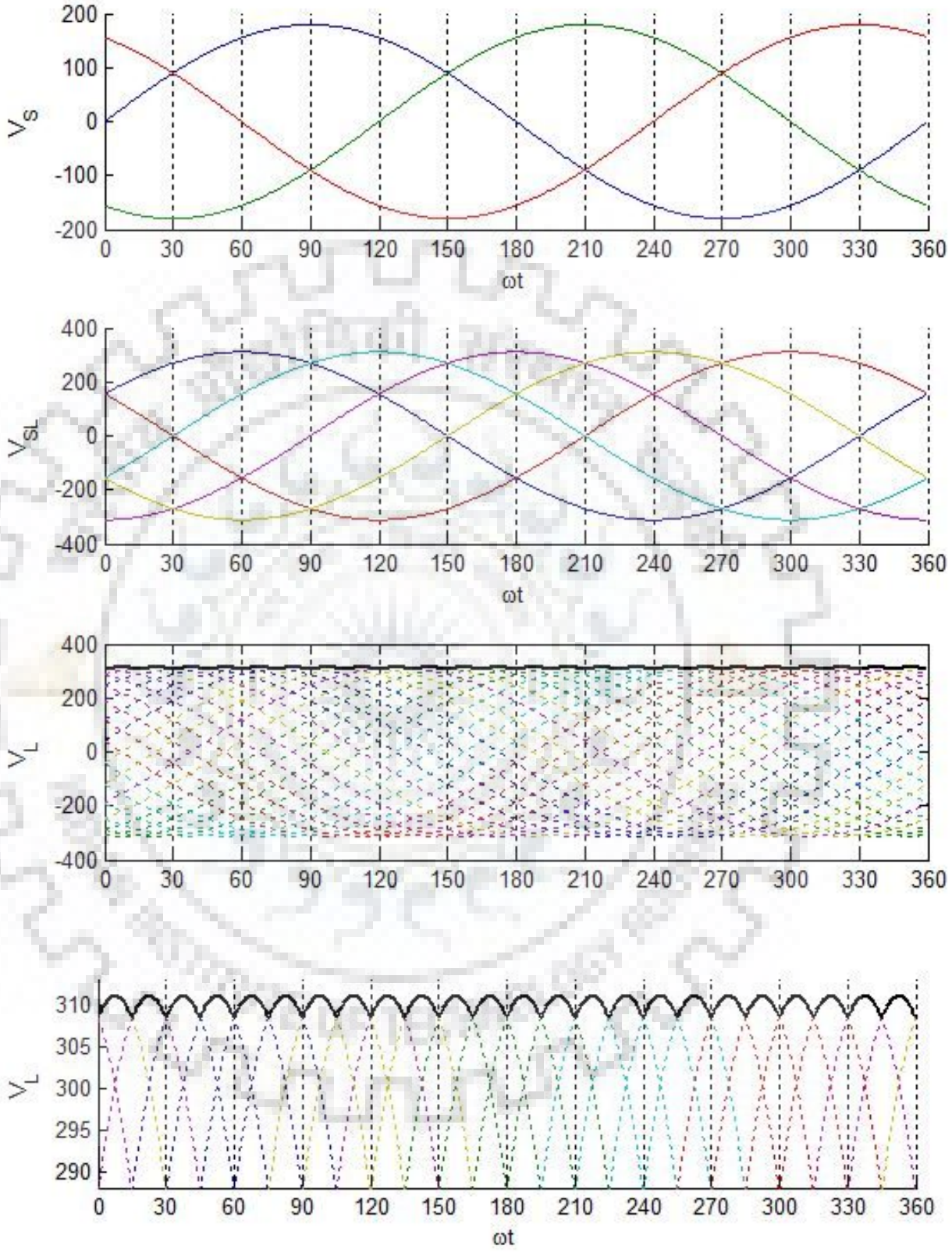

Fig 4.18. On constant current load the output of 24 pulse converter

If the secondary voltage are known, voltages of converters can be eshown in these ways. The secondary winding voltages can be shown as,

$$V_A = K_1 V_A + K_4 V_A$$
$$K_1 + K_4 = 1$$
$$V_{A1} = K_1 V_a + K_2 V_b - K_3 V_b$$
$$V_{A2} = K_1 V_a - K_2 V_b + K_3 V_a$$
$$V_{A3} = V_{A2} \angle 15°$$
$$V_{A4} = V_{A1} \angle -45°$$

We obtain solving these equations,

$K_1 = 0.7029$ $K_2 = 0.1507$ $K_3 = 0.2912$ $K_4 = 0.2132$ $K_5 = 0.2971$ (4.27)

POWER RATINGS

$$P_d = V_d I_d$$
$$V_d = \frac{3}{\pi} V_{ML}$$
$$= \frac{3\sqrt{2}\sqrt{3}}{\pi} V_S$$
$$V_S = \frac{\pi}{3\sqrt{6}} V_d$$

(4.28)

VOLTAGE RATINGS

$$V_{ph} = K_1 V_S = 0.7029 V_S$$
$$V_{zig1} = K_2 V_S = 0.1507 V_S$$
$$V_{zig2} = K_3 V_S = 0.2912 V_S$$
$$V_{ph1} = K_5 V_S = 0.2132 V_S$$
$$V_{in} = K_4 V_S = 0.2971 V_S$$

(4.29)

CURRENT RATINGS

$$i_a = i_{A1} + i_{A2} + i_A + i_{A3} + i_{A4}$$
$$i_b = i_{B1} + i_{B2} + i_B + i_{B3} + i_{B4}$$
$$i_c = i_{C1} + i_{C2} + i_C + i_{C3} + i_{C4}$$

(4.30)

In phase A

$$K_4 i_a + K_1 i_A + K_3 i_{C1} + K_3 i_{B4} + K_2 i_{C1} + K_2 i_{B4} + K_2 i_{C2} + K_2 i_{B3} = 0$$

(4.31)

Similarly in phase C and in phase B.

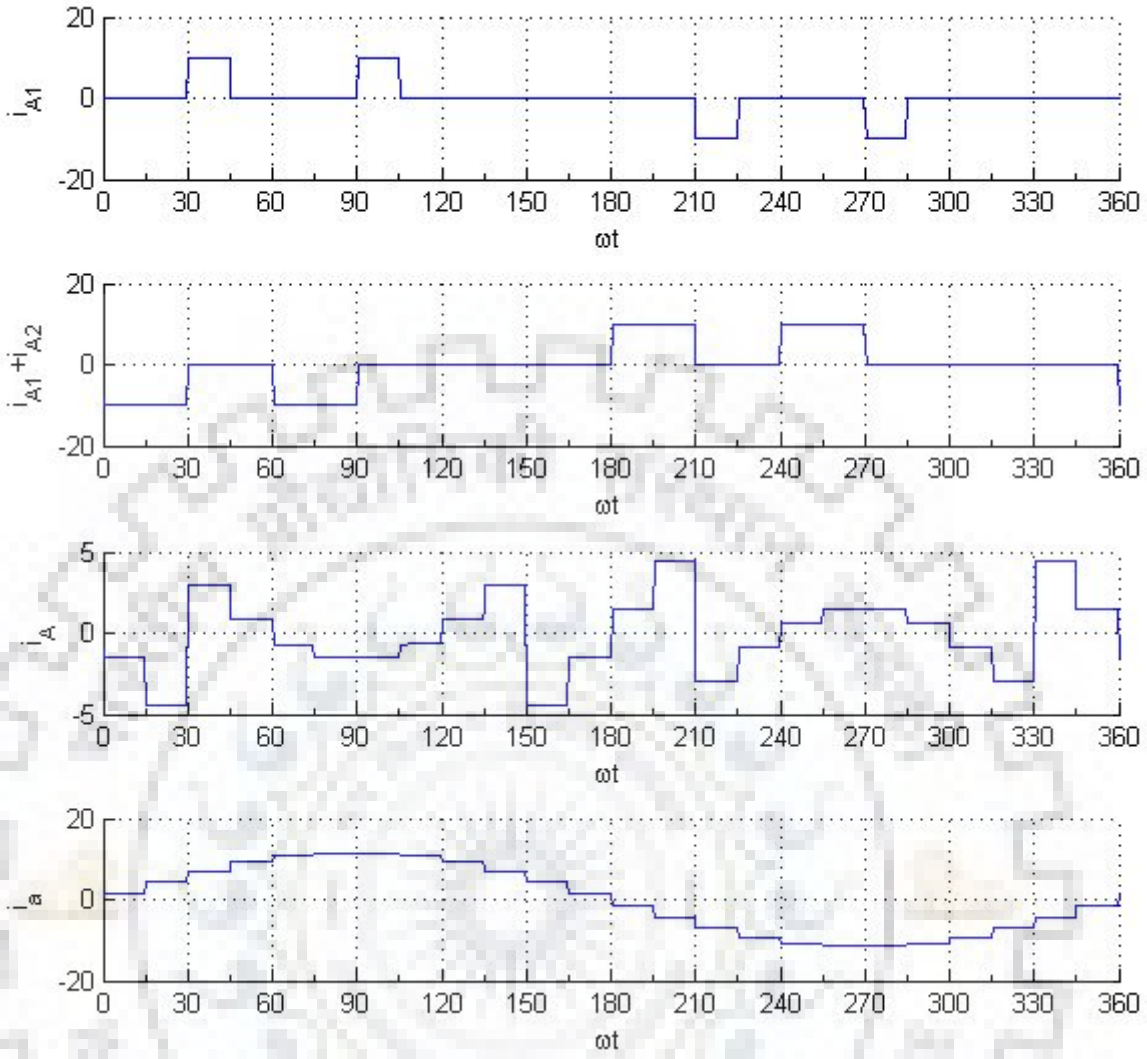

Fig 4.19. The current in various windings of fork transformer on constant curent load

Calculating these on constant current load whose result is as shown in fig 4.19., we get the following values,

$$(i_A)_{rms} = 0.0237\ I_d$$
$$(i_a)_{rms} = 0.8195\ I_d$$
$$(i_{A1})_{rms} = 0.4075\ I_d$$
$$(i_{A2})_{rms} = 0.4075\ I_d$$
$$(i_{A3})_{rms} = 0.4075\ I_d$$
$$(i_{A4})_{rms} = 0.4075\ I_d$$

(4.32)

From equations (4.27), (4.28) and (4.31), we get,

$I_{zig1} = (i_{A1})_{rms} = 0.4075\ I_d$ $\quad V_{zig1} = K_3 V_S = 0.2912 V_S$

$I_{zig2} = (i_{A1}+i_{A2})_{rms} = 0.5762\ I_d$ $\quad V_{zig2} = K_2 V_S = 0.1507 V_S$

$I_{ph} = (i_A)_{rms} = 0.0237\ I_d$ $\quad V_{ph} = K_1 V_S = 0.7029 V_S$

$I_{ph1} = (i_{A2})_{rms} = 0.4075\ I_d$ $\quad V_{ph1} = K_4 V_S = 0.2132 V_S$

$I_{in} = (i_a)_{rms} = 0.8195\ I_d$ $\quad V_{in} = K_5 V_S = 0.2971 V_S$

And,

$$KVA_{zig1} = I_{zig1}V_{zig1} = 0.1187P_d$$
$$KVA_{zig2} = I_{zig2}V_{zig2} = 0.0827P_d$$
$$KVA_{ph} = I_{ph}\ V_{ph} = 0.1666P_d$$
$$KVA_{ph1} = I_{ph1}\ V_{ph1} = 0.0869P_d$$
$$KVA_{in} = I_{in}V_{in} = 0.2435P_d$$

$$KVA\ total = \frac{1}{2}\ [6\times KVA_{zig1} + 6\times KVA_{zig1} + 3\times KVA_{ph} + 6\times KVA_{ph1} + 3\times KVA_{in}]$$
$$= 0.492\ P_d \qquad (4.33)$$

This mean, it requires 49.2 % of load for transformer.

The MATLAB model of 24 pulse fork converter is shown in fig.4.20.

- It is realised through multi winding transformer with appropriate values.

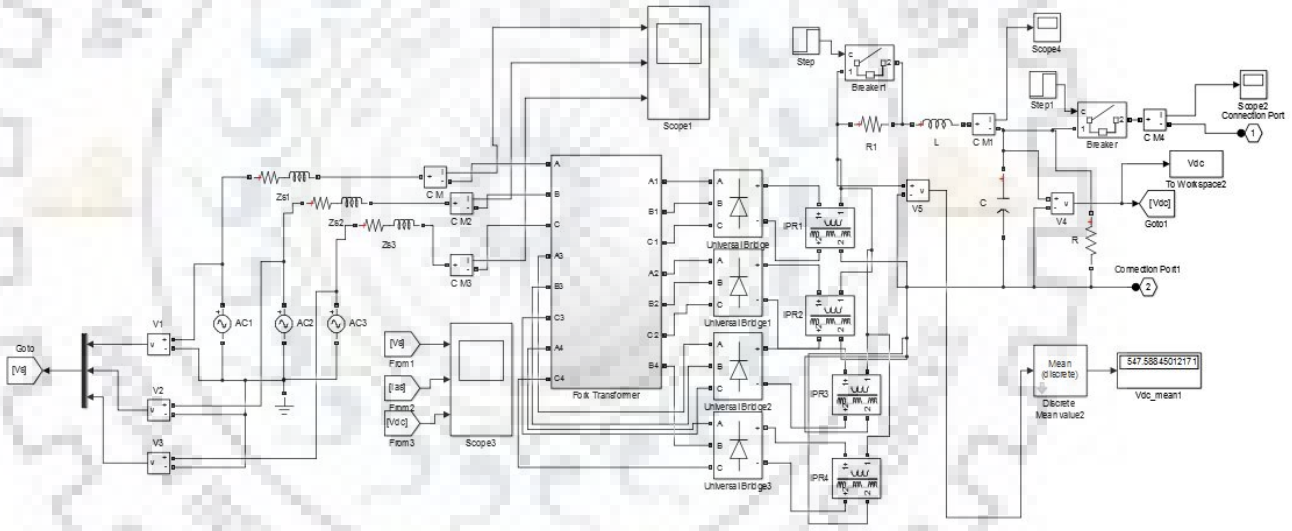

Fig 4.20 MATLAB model of 24 pulse AC-DC converter

Each multi winding transformer has single phase transformer, one for each primary, secondary star and secondary delta of a single phase. Each of these windings are then connected accordingly.

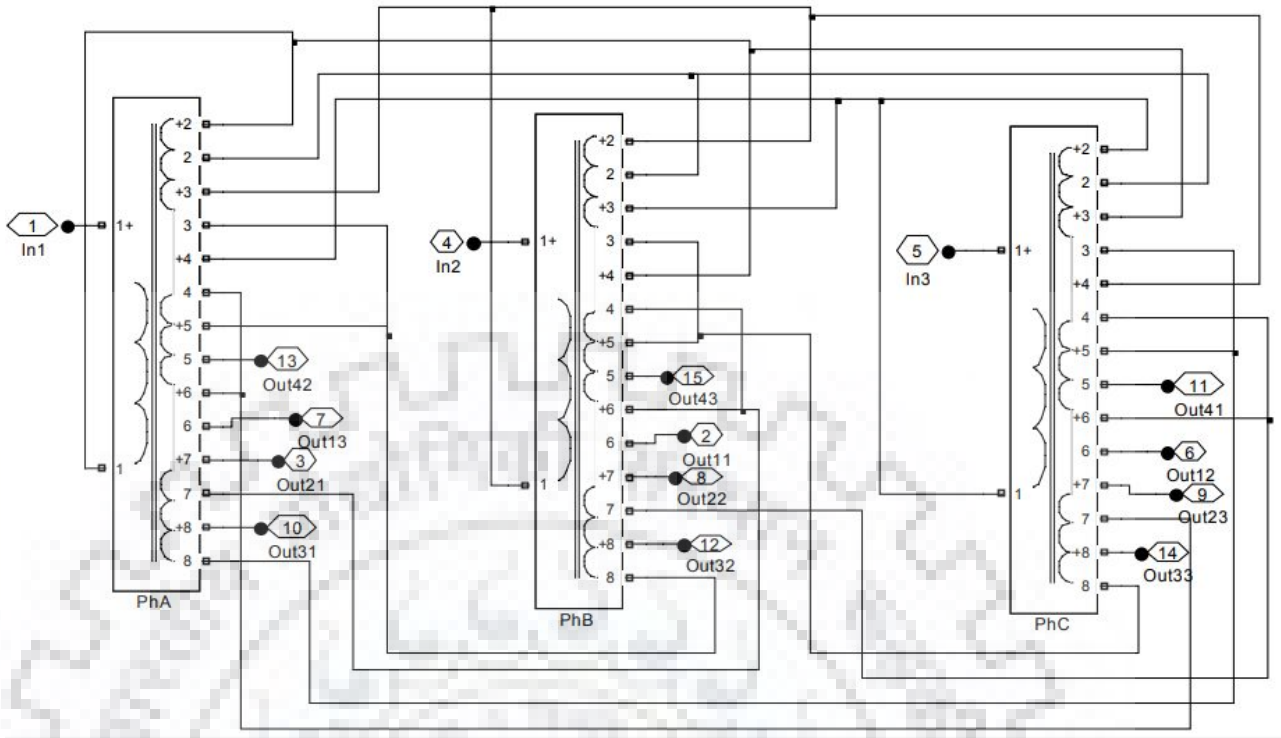

Fig 4.21. MATLAB model of fork auto transformer

CHAPTER V

RESULTS AND CONCLUSION

The three topology has been designed and investigated into their merits. The topology can also be compared with 6 pulse uncontrolled converter for comparing their performance. The starting dynamics and load perturbation of the machine fed by the different topologies have been studied and their respective THD at full load observed.

The results of the investigations are:

5.1.1. DELTA - STAR-DELTA CONNECTED TWELVE PULSE UNCONTROLLED CONVERTER FED VECTOR COTROLLED INDUCTION MOTOR DRIVE

The Fig 5.1. to fig 5.3. Shows the dynamic response of the drive

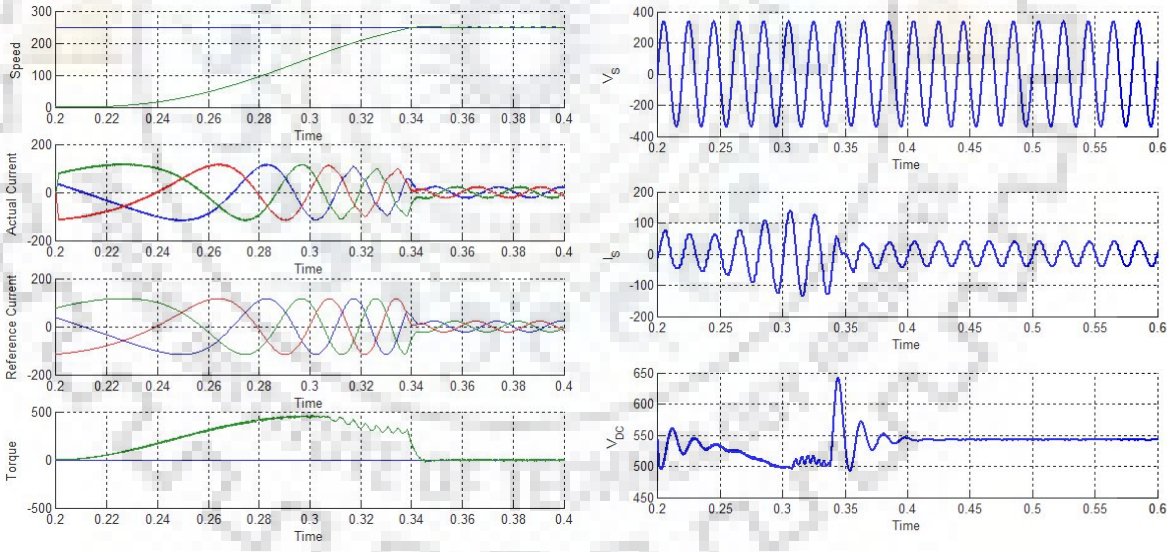

(a) (b)

Fig 5.1 Starting response of 12 pulse uncontrolled AC-DC converter fed VCIMD

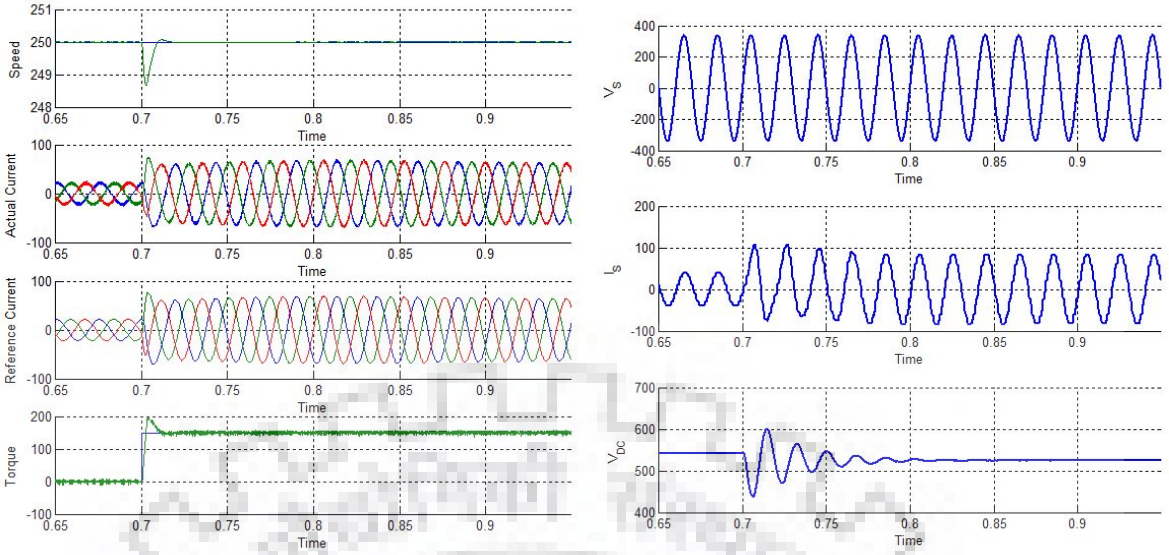

(a) (b)

Fig 5.2 Response at Load application of 12 pulse uncontrolled AC-DC converter fed VCIMD

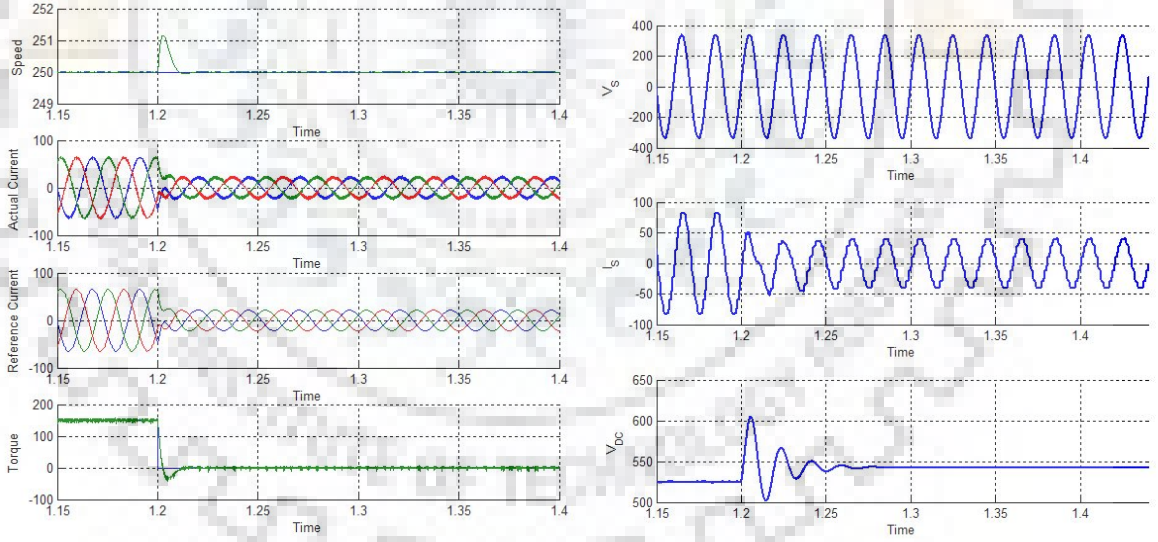

(a) (b)

Fig 5.3 Response at Load removal of 12 pulse uncontrolled AC-DC converter fed VCIMD

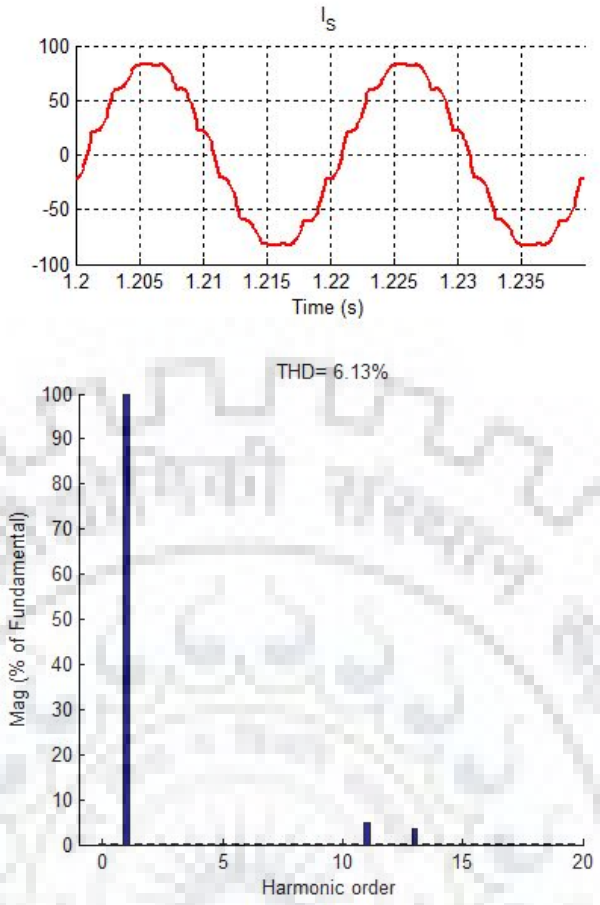

Fig. 5.4. THD analysis of Supply current

There is an improvement in the wave shape of input current over 6 pulse converter and the THD is observed to be 6.13%. The harmonic analysis in Fig 5.4 shows that there are dominating 11th and 13th harmonics. The voltage ripple comes to be 3.63 V peak to peak and % RF is obtained 0.68.

5.1.2. FORK CONNECTED AUTO-TRANSFORMER BASED 12 PULSE UNCONTROLLED CINVERTER FED VECTOR COTROLLED INDUCTION MOTOR DRIVE

The Fig 5.4. to fig 5.6. Shows the dynamic response of the drive

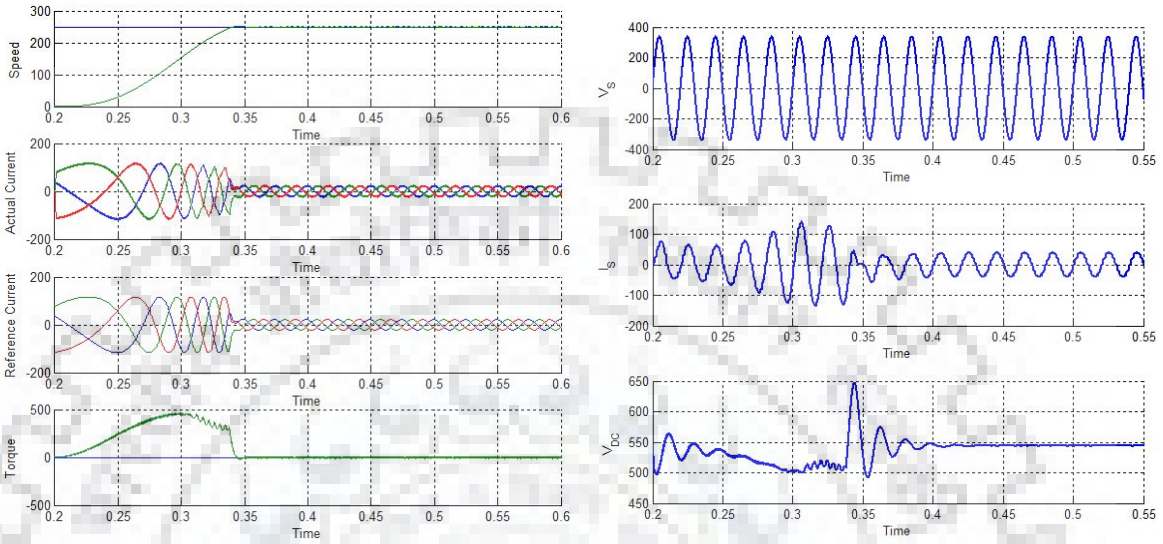

(a) (b)

Fig 5.4 Starting response of fork based 12 pulse AC-DC converter fed VCIMD

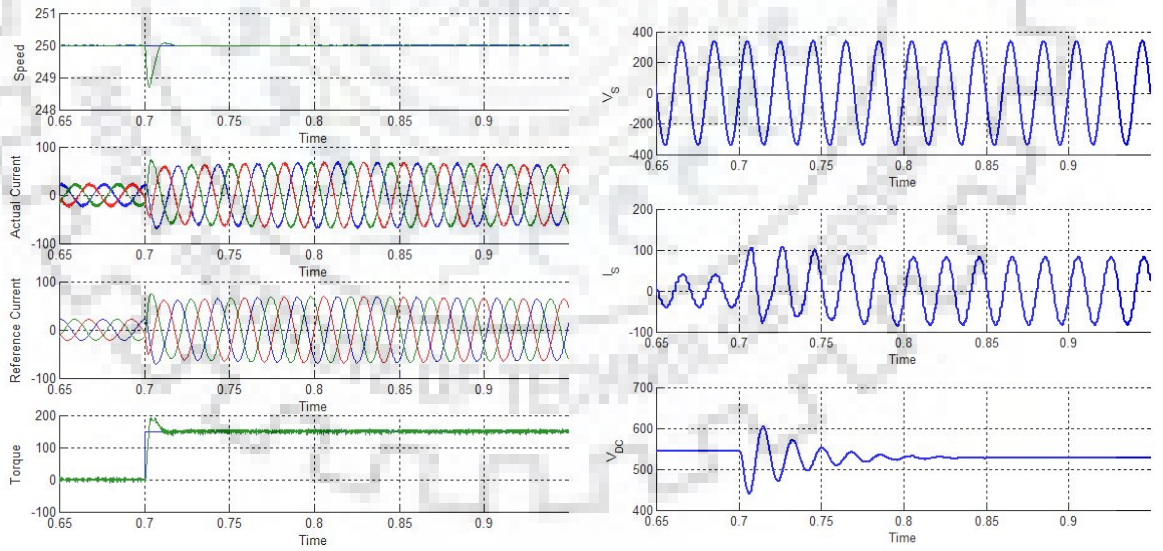

(a) (b)

Fig 5.5 Response at Load application of fork based 12 pulse AC-DC converter fed VCIMD

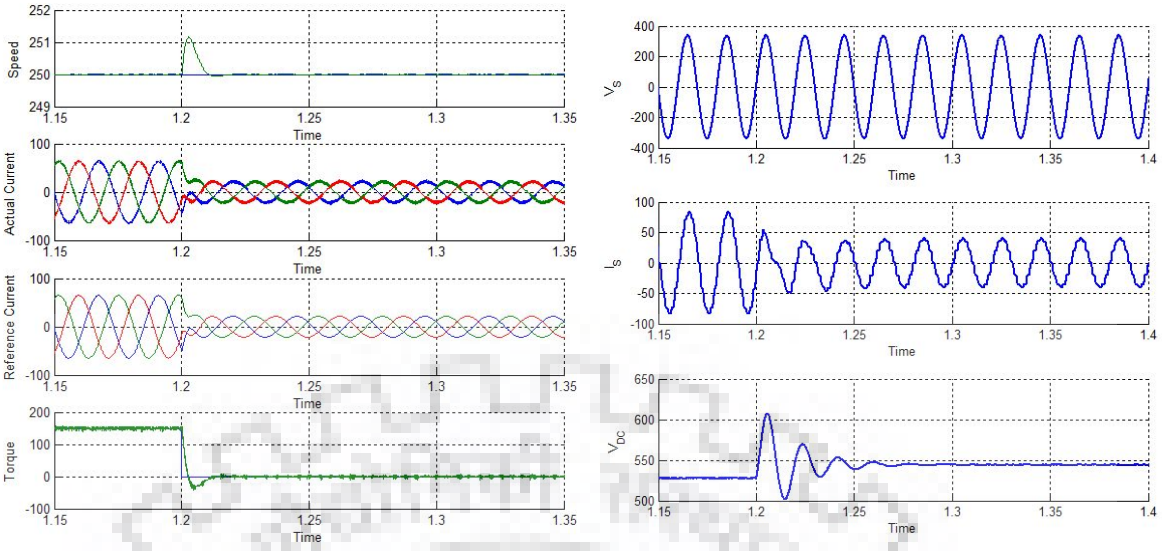

(a) (b)

Fig 5.6 Response at Load removal of fork based 12 pulse AC-DC converter fed VCIMD

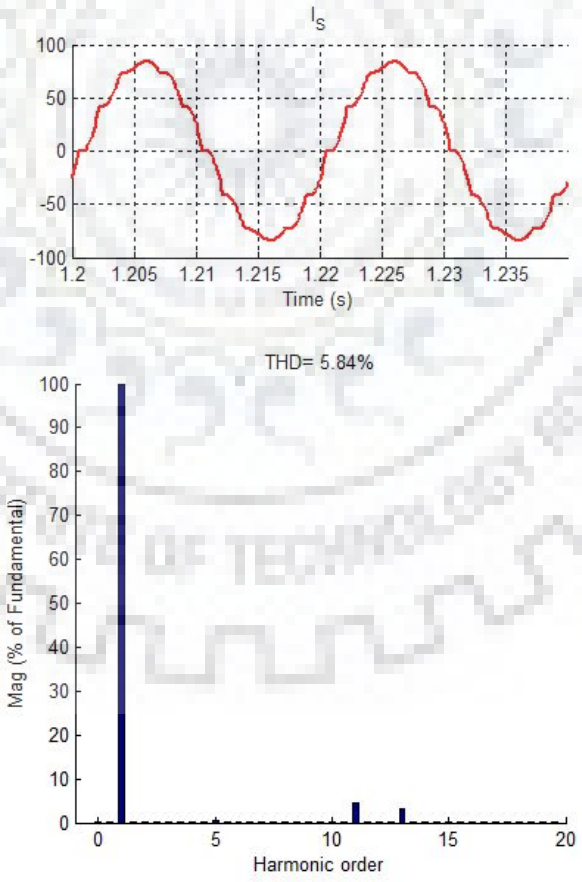

Fig 5.7. THD analysis of Supply current

There is not much improvement in the wave shape of input current over 12 pulse converter and the THD is observed to be 5.84%. The harmonic analysis in Fig 5.4 shows that there are still dominating 11th and 13th harmonics.

As we have invastigated in the design of the two transformer, even though the THD is not much different, the KVA requirement of Fork transfomrer is much less than the isolated Delta/Star-Delta transformer.

5.1.3. FORK CONNECTED AUTO-TRANSFORMER BASED 12 PULSE CINVERTER FED VECTOR COTROLLED INDUCTION MOTOR DRIVE

The Fig 5.7. to fig 5.9. Shows the dynamic response of the drive

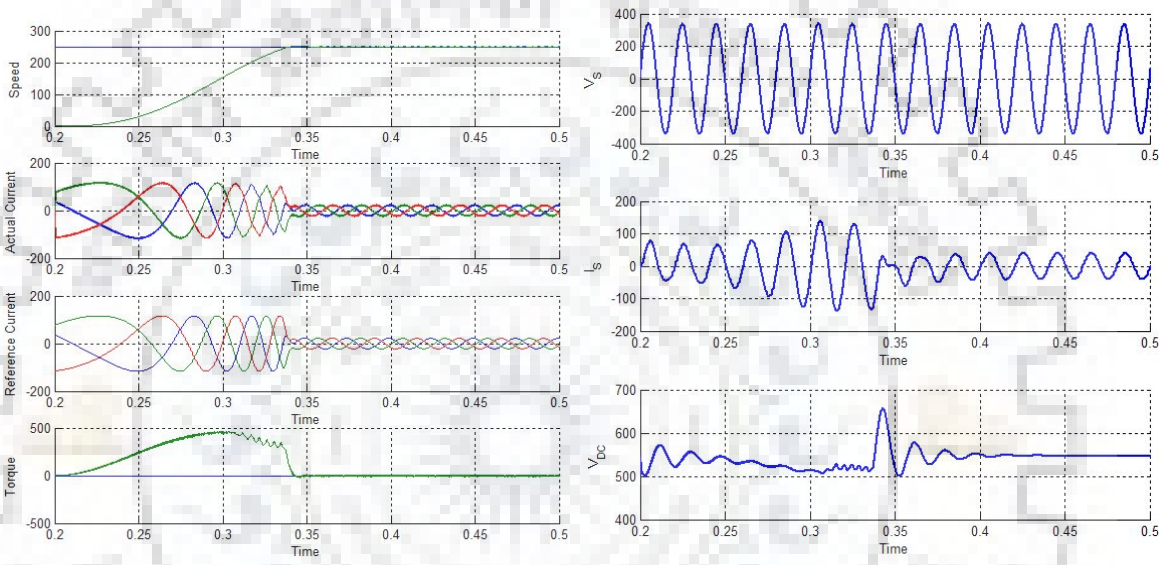

(a) (b)

Fig 5.7. Starting response of fork based 24 pulse AC-DC converter fed VCIMD

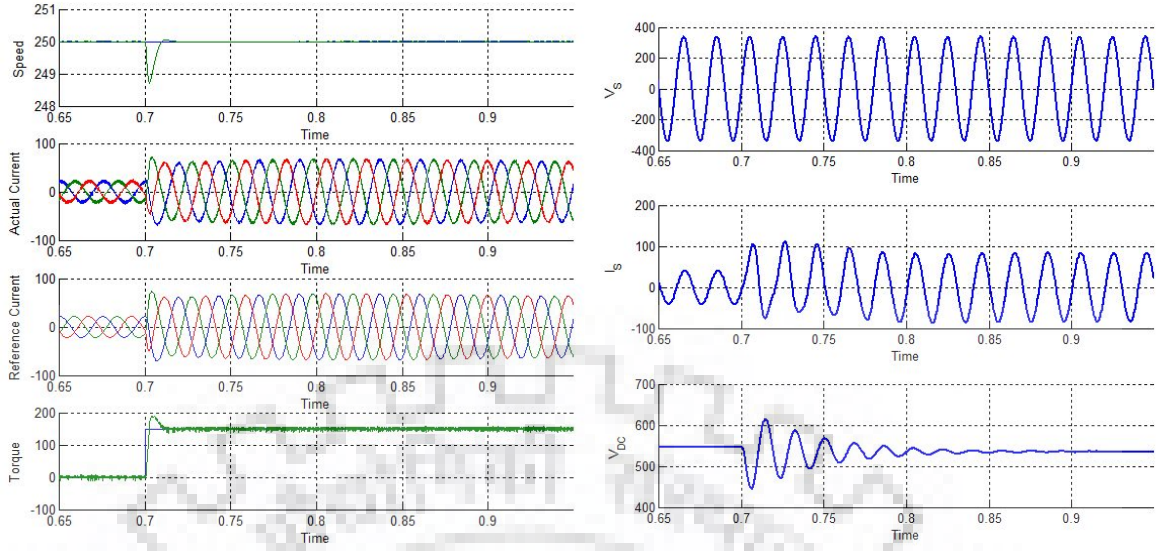

(a) (b)

Fig 5.8. Response at Load application of fork based 24 pulse AC-DC converter fed VCIMD

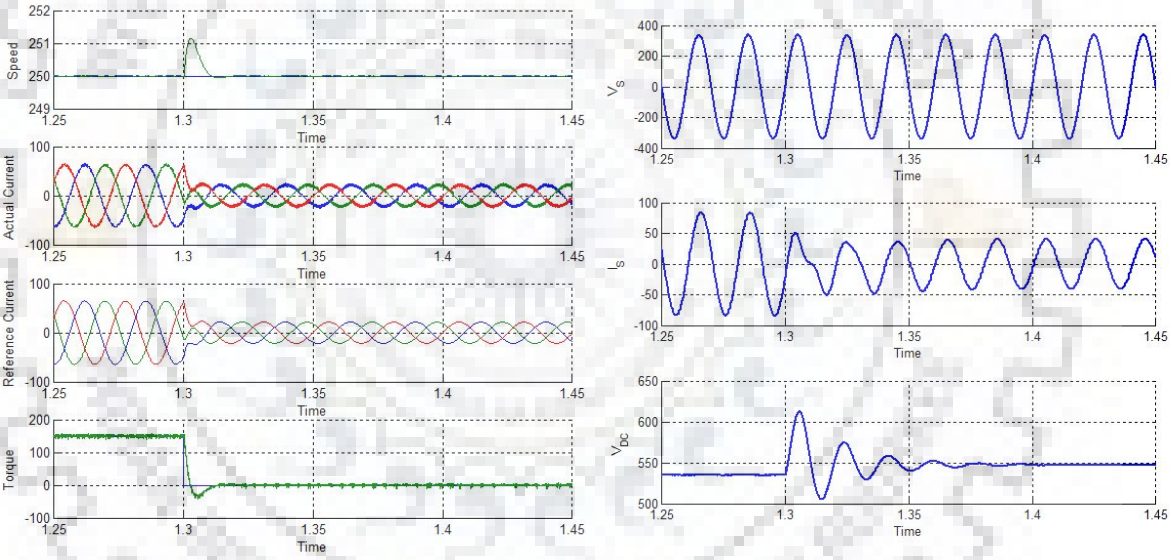

(a) (b)

Fig 5.9. Response at Load removal of fork based 24 pulse AC-DC converter fed VCIMD

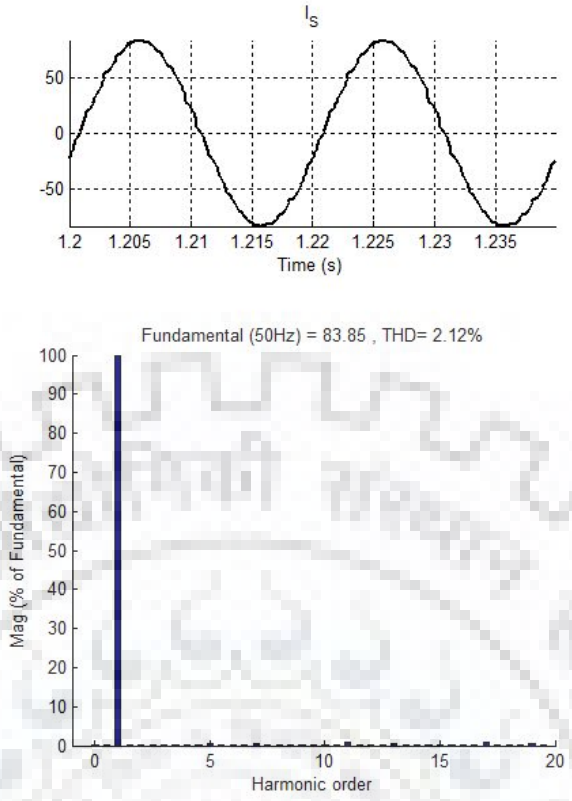

Fig 5.7. THD analysis of Supply current

There is an improvement in the wave shape of input current over 12 pulse converters and the THD is observed to be 2.12%. The harmonic analysis in Fig 5.4 shows that there are the 11th and 13th harmonics are suppressed.

As we have invastigated in the design of the three transformer, the result sre summrised in the TABLE I.

The magnetic rating of the three topologies is given in TABLE II.

TABLE I

Topology	Vs	Is	THD	Vdc	PF	DF	DPF	%RF	Vripple
6-pulse	239.3	55.46	24.062	536.16	0.9393	0.971	0.9674	4.313	23.12
12 pulse Dyd	239.2	59.74	6.122	527.93	0.9634	0.9981	0.9652	6.964	36.77
12 pulse Fork	239.2	58.84	5.84	531.74	0.9682	0.9699	0.9983	8.792	46.75
24 pulse	239.2	60.52	2.12	542.03	0.9735	0.9998	0.9738	0.7975	4.323

TABLE II

S.no.	Topology	Main transformer rating (% of load)	Interphase transformer rating (% of load)	Total Magnetic Loading
1	12 pulse Dyd	102.9	7.6	110.5
2	12 pulse Fork	28.68	10.35	48.795
3	24 pulse fork	49.2	7.36	56.56

5.1.4. CONCLUSION

The aim of this investigation is to improve the power quality at the supply end to feed a VCIMD system. On the basis of results obtained, it can be said that by using more than six numbers of pulses the performance of AC-DC converters in terms of power quality is improved. The distortion in input supply current is decreased by using multi-pulse converters and the quality of DC link voltage has been improved as well. Not much change in Power factor (PF) of the system has been seen in any of the cases. The waveform of the input current is improved from non-sinusoidal to close to sinusoidal.

CAPTER VI
CONCLUSION AND FUTURE SCOPE

6.1 CONCLUSION

For simle application PI is used, for intelligent application fuzzy is used. Fuzzy Logic Control suffers with disadvantages such as steady state speed on load. So, the use of intelligent controller which incorporate both features of PI and FL as a function of the speed error for taking the best of both controller.

The aim of this investigation is to improve the power quality at the supply end to feed a VCIMD system. On the basis of results obtained, it can be said that by using more than six numbers of pulses the performance of AC-DC converters in terms of power quality is improved. The distortion in input supply current is decreased by using multi-pulse converters and the quality of DC link voltage has been improved as well. Not much change in Power factor (PF) of the system has been seen in any of the cases. The waveform of the input current is improved from non-sinusoidal to close to sinusoidal.

6.2 FUTURE SCOPE OF WORK

For future scope, the speed sensor iself can be removed and speed can be sestimated throught the current with various modelling. Another scope will be to use hierarchial fuzzy or adaptive fuzzy speed controller, SMC, Fuzzy SMC etc.

Matrix converter, Current source inverter can be used to fed the induction motor.

For power quality improvement various other topologies such as delta polygon, delta-doble polygon-delta, delta hexagon can be investigated to find their performances.

APPENDIX

Specification of the induction motor considered in this report.

Cage Induction Motor

30 HP, 3 - phase, 4 - pole, Y - connected 415V, 50 Hz, $R_s = 0.251\ \Omega$, $R_r = 0.249\ \Omega$, $L_m = 0.0416H$, $L_{ls} = 0.001397$ H, $J = 0.305$ Kgm^2

Speed Contoller

PI controller and Intelligent Controller Parameters $K_P = 360$; $K_I = 50$.

BIBLIOGRAPHY

[1] W. Leonard, "Control of Electric Drives", New Delhi, Narosa Publications, 1985.

[2] P.C. Krause, Electrical Machines, Prentice Hall, 1985.

[3] J.M.D. Murphy and F.G. Turnbull, Power Electronic Control of AC Motors, Oxford Pergamon Press, 1988.

[4] P.Vas, Vector Control of AC Machines, Oxford University Press, 1990.

[5] I. Boldea and S.A. Nasar, Vector Control of AC Drives, Florida, CRC Press, 1992.

[6] P. Vas, Sensorless Vector Control and Direct Torque Control , Oxford University Press, New York, 1998.

[7] Muhammad H. Rashid, Power Electronics Circuits, Devices and Applications, Pearson Education third edition,2004.

[8] P. C. Krause and C. H. Thomas, " Simulation of Symmetrical Induction Machinery", IEEE Trans. On Power Apparatus and Systems, Vol.PAS 84, No. 11, Nov. 1965.

[9] D. A. Paice, Power Electronic Converter Harmonics: Multipulse Methods for Clean Power, New York:IEEE Press, 1996.

[10] Sathi Kumar. S and Vithajathil. Joseph, "Digital SimulAion of Field Oriented Control of Induction Motor", IEEE Transactions on Industrial Electronics, Vol. IE-31, Issue 2, May 1984, pp. 141-148.

[11] I. Ludtke, and M. G. Jayne, " A Comparative Study Of High Performance Speed Control Strategies For Voltage Sourced PWM Inverter Fed Induction Motor Drives", Conference Publication No. 412, IEE, September 1995.

[12] D. Telford, M. Dunnigan, and B. W. Williams, " A Comparison of vector control and direct torque control of an induction machine", IEEE Trans. Power Electronics, pp. 421-426, 2000.

[13] D. Casadei, F. Profum, G.serra, and A. Tani, " The Use of Matrix Converters in Direct Torque Control of Induction Machines", IEEE Trans. On Industrial Electronics, Vol. 48, No. 6, Dec. 2001.

[14] D.A. Paice, "Wye connected 3-phase to 9-phase autotransformer with reduced winding currents," U.S. Patent No. 6,191,968 B1, Feb. 20, 2001.

[15] T. A. Wolbank, A. Moucka, and J. L. Machl, "A comparative study of field oriented control and direct torque control of induction motors reference to shaft-sensorless control at low and zero speed", IEEE International, pp. 391-396, Oct 2002.

[16] Bhim Singh and Sumit Ghatak Choudhuri," Fuzzy Logic Based Speed Controllers for Vector Controlled Induction Motor Drive" , IETE Journal of Research, Vol. 48, No. 6,pp. 441-447, Nov.-Dec., 2002.

[17] B. Singh, G. Bhuvaneshwari and Vipin Garg, "A Twelve-Phase AC-DC Converter for Power Quality Improvements in Dirtect Torque Controlled Induction Motor Drives", in Proc. of Conf. IEEE- ICIEA 2006, May 2006, pp 257-263.

[18] Bhim Singh and Sanjay Gairola, "A Fork Connected Transformer Based 24-Pulse AC-DC Converter", IEEE International Conference on Industrial Technology, 2006

[19] Bhim Singh, G. Bhuvaneswari, Vipin Garg, "Harmonic Mitigation Using 12-Pulse AC–DC Converter in Vector-Controlled Induction Motor Drives" , IEEE Transactions On Power Delivery, Vol. 21, No. 3, July 2006

[20] Bhim Singh and Sumit Ghatak Choudhuri, "Speed Sensorless Control of Vector Controlled Induction Motor Drive", The ICFAI Univ. Journal, Vol. 1, No. 2, 2008.

[21] Bhim Singh, Sanjay Gairola, Brij N Singh, Ambrish Chandra, Kamal Al-Haddad, "Multipulse AC–DC converters for improving power quality: a review", IEEE Transactions on Power Electronics, Vol. 23, Issue. 1, 2008.

[22] Suneel Kumar Agrawal, Sumit Ghatak Choudhuri, "Simulation of Vector Controlled Induction Motor Drive in MATLAB for Various Applications: A Comparative Study", Proc. Michael Faraday IET International Summit-2015, pp. 533-54, 12–13 Sept, 2015.

[23] Vanshika Jindal, Laxman Singh, Prem Prakash Dudi, Sumit Ghatak Choudhuri, "Operation of Induction Motor in Vector Controlled Mode with variation in Speed Controller logic: A comparative study", Electrical Computer and Electronics Engineering (UPCON) 2016 IEEE Uttar Pradesh Section International Conference on, pp. 519-524, 2016.